JOC The Journal of Organic Chemistry

Article

pubs.acs.org/joc

Palladium(II)-Catalyzed Cycloisomerization of Substituted 1,5-Hexadienes: A Combined Experimental and Computational Study on an Open and an Interrupted Hydropalladation/Carbopalladation/β-Hydride Elimination (HCHe) Catalytic Cycle

Björn Nelson,* Sonja Herres-Pawlis, Wolf Hiller, Hans Preut, Carsten Strohmann, and Martin Hiersemann*

Fakultät Chemie, Technische Universität Dortmund, 44227 Dortmund, Germany

Supporting Information

ABSTRACT: The Pd^{II}-catalyzed cycloisomerization of 3-alkoxycarbonyl-3-hydroxy-substituted 1,5-hexadienes has been studied experimentally and computationally. Experimentally, the reaction is characterized by a rapid room temperature formation of monomeric as well as dimeric cycloisomerization products using the commercially available precatalyst $[(CH_3CN)_4Pd](BF_4)_2$. In situ NMR measurements indicate the initial kinetic advantage of the desired cycloisomerization pathway to methylene cyclopentanes; however, double bond isomerization, elimination, and dimer formation are competitive undesired pathways. Evaluation of the obtained product structures by NMR spectroscopy and X-ray crystallography indicates that the sole determinant for the monomer/dimer ratio is the regioselectivity of the initial hydropalladation in favor of the allylic (monomer formation) or the homoallylic double bond (dimer formation). In order to account for the experimental results, we propose the coexistence of two product-forming catalytic cycles, an open, monomer generating, as well as an interrupted and redirected, dimer generating, hydropalladation/carbopalladation/β-hydride elimination (HCHe) process. Results from computational studies of the proposed competing catalytic cycles are supportive to our mechanistic hypothesis and pinpoint the pivotal importance of Pd^{II}-hydroxo-chelate complexes for the reactivity−stability interplay of on- and off-pathway intermediates.

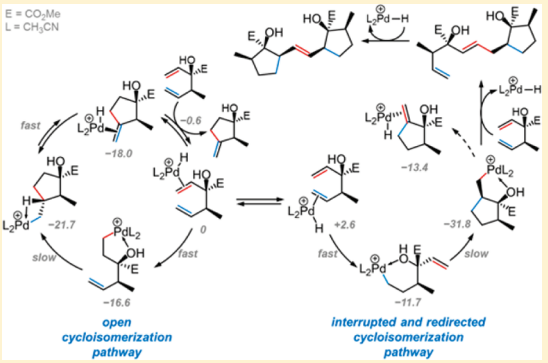

INTRODUCTION

Substituted cyclopentanes represent a common structural motive in secondary natural products and/or molecules with interesting pharmacological properties. Therefore, a plethora of synthetic strategies for the synthesis of cyclopentane building blocks is available.[1] The transition-metal-catalyzed cycloisomerization of linear 1,*n*-dienes, -enynes, and -diynes is a proven synthetic method for the construction of functionalized carbocycles;[2] the cycloisomerization is particularly attractive because it creates, perfectly atom-economic, structural complexity from easily available acyclic molecules of much lower molecular complexity.[3] 2,2-Diallyl malonates have been used as "benchmark" substrates for the metal-catalyzed cycloisomerization of 1,6-dienes.[4−9] In stark contrast, however, only a small number of examples exist for the cycloisomerization of 1,5-hexadienes, although this reaction has its roots in the middle of the last century.[10−12] For instance, Livinghouse has reported the cycloisomerization of a functionalized 1,5-hexadiene to the corresponding methylene cyclopentane in the presence of a Ti-catalyst[8b] (Scheme 1, Ti^{II}). Examples for the cycloisomerization of unsubstituted 1,5-dienes with late transition-metals where initially revealed by Wilke,[13] Keim,[14] and Walther[15] (nickel-catalysis). Widenhoefer subsequently reported the cycloisomerization of substituted 1,5-hexadienes by a cationic (phen)Pd^{II}-complex (Scheme 1, $Pd^{II}\oplus$).[16]

In comparison to 1,6-heptadienes, 1,5-hexadienes are more challenging substrates because they are generally less reactive and frequently require elevated reaction temperatures to enforce conversion. For instance, the cycloisomerization of dimethyl allyl(propenyl)malonate by $(t\text{-BuCN})_2PdCl_2$ required forcing conditions (110 °C, 72 h), and five different cycloisomerization products were detected (Scheme 1, Pd^{II}).[17] Extensive experimental investigations by Lloyd-Jones revealed that 1,5-hexadienes, which were formed as byproducts during the cycloisomerization 1,6-heptadienes, act as powerful "Pd−H-traps" and cycloisomerization inhibitors, even if present in only catalytical amounts (<5%).[18,19] A further restriction arises from the experimental observation that under the conditions of the cycloisomerization, the desired methylene cyclopentanes are converted to methyl cyclopentenes by subsequent double-bond isomerization.

Despite the looming difficulties in terms of reactivity and chemo- and regioselectivity, we embarked to establish conditions

Received: March 2, 2012

   dx.doi.org/10.1021/jo3004088 | J. Org. Chem. XXXX, XXX, XXX−XXX

Scheme 1. Cycloisomerization of 1,5-Dienes: Literature Precedence

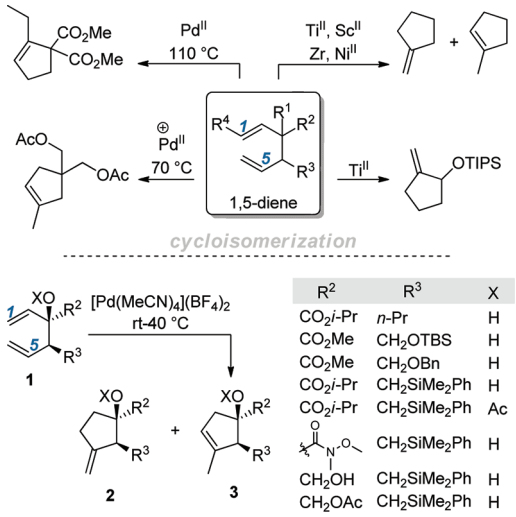

for the cycloisomerization of highly functionalized 1,5-hexadienes **1**, featuring heterotopic double bonds, to methylene cyclopentanes **2**. Our initial study revealed the usefulness of the commercially available catalyst $[Pd(MeCN)_4](BF_4)_2$ (Scheme 1, bottom),[20,21] but the synthetic value of the procedure was hampered by a close competition between various reaction pathways.

In this article, we report the details of a combined experimental and computational endeavor that was undertaken to compile evidence and information on the mechanistic details of the Pd^{II}-catalyzed cycloisomerization of 1,5-hexadienes **1**.

RESULTS AND DISCUSSION

Experimental Studies. We embarked on this part of our study with a catalyst screening; selected results for a single substrate are summarized in Table 1. When subjecting the 1,5-hexadiene **1a**[20] to $[Pd(MeCN)_4](BF_4)_2$ in CH_2Cl_2 at room temperature, we obtained the desired cycloisomerization product, methylene cyclopentane **2a**, in encouraging yield (Table 1, entry 1). Optimization of the reaction conditions in terms of temperature (40 °C) and time (3.5 h) then delivered **2a** with 68% yield, albeit with slightly eroded chemoselectivity (**2a**/**3a** = 91/9) (Table 1, entry 2). The presence of molecular sieves (ms) seems to efficiently suppress the cycloisomerization reaction, even at elevated temperatures (Table 1, entry 3).[22] Attempts to modulate the reactivity of the catalyst system by the addition of monodentate phosphines (0.05 equiv of PCy_3) led to inferior yields and selectivities (Table 1, entry 4); likewise, $[Pd(dppp)(PhCN)_2](BF_4)_2$ was not competent to catalyze the cycloisomerization (Table 1, entry 5); notably, performing the reaction in toluene at reflux led to the formation of significant amounts of the α-keto ester **4** by an oxy-Cope rearrangement (Table 1, entry 6).[23] Switching to $(MeCN)_2PdCl_2$, no cycloisomerization product was obtained; again, at higher reaction temperatures (70 °C) the formation of **4** could be detected (Table 1, entries 7 and 8). These observations underline the importance of the development of a low-temperature catalyst system. In an attempt to accomplish the cycloisomerization of **1a** using a purposeful in situ generated L_nPd-H catalyst, an equimolar mixture of $(MeCN)_2PdCl_2$ and Et_3SiH according to Lloyd-Jones[17] was employed, unfortunately, without any notable success (Table 1, entry 9). Recruitment of $[Pd(\eta^3\text{-allyl})(MeCN)_2](OTf)$,[24] which was shown to be an active catalyst for the cycloisomerization of 1,6-heptadienes,[9i] resulted in the formation of only small amounts of the cycloisomerization product **2a**, even after prolonged heating (Table 1, entry 10). $Pd(\eta^3\text{-allyl})(MeCN)_2](BF_4)$,[25] containing a weakly coordinating counterion, triggered cycloisomerization but is less reactive and selective than $[Pd(MeCN)_4](BF_4)_2$ (Table 1, entries 2 and 11).

Conceptual Catalytic Cycle for the Cycloisomerization.[26] Guided by the accepted mechanism for the Pd^{II}-catalyzed cycloisomerization of 1,6-dienes,[2,16,17] we initially proposed a conceptual catalytic cycle, which is triggered by the in situ

Table 1. Screening Precatalysts and Conditions for the Cycloisomerization of 1a[a]

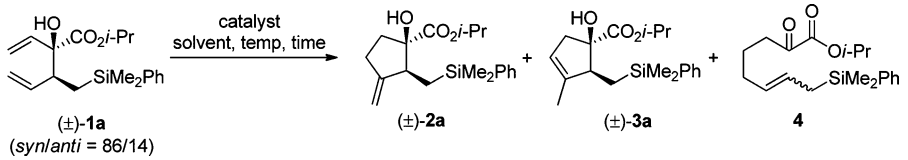

entry	catalyst, additives (equiv)	solvent	temp (°C)	time (h)	yield[b] (%) (**2a**/**3a**)[c]
1	$[Pd(MeCN)_4](BF_4)_2$ (0.05)	CH_2Cl_2	rt[d]	19	50 (95/5)
2	$[Pd(MeCN)_4](BF_4)_2$ (0.05)	CH_2Cl_2	40	3.5	68 (91/9)
3	$[Pd(MeCN)_4](BF_4)_2$ (0.05), ms (4 Å)	$(CH_2Cl)_2$	40	4	no reaction
4	$[Pd(MeCN)_4](BF_4)_2$ (0.05), PCy_3 (0.05)	$(CH_2Cl)_2$	70	19	44 (86/14)
5	$[Pd(dppp)(PhCN)_2](BF_4)_2$ (0.05)	CH_2Cl_2	75	19	no reaction
6	$[Pd(dppp)(PhCN)_2](BF_4)_2$ (0.05)	toluene	110	19	(80)[e,f]
7	$(MeCN)_2PdCl_2$ (0.05)	$(CH_2Cl)_2$	40	72	no reaction
8	$(MeCN)_2PdCl_2$ (0.05)	$(CH_2Cl)_2$	70	72	79 (0/30/70)[e,f,g]
9	$(MeCN)_2PdCl_2$ (0.05), Et_3SiH (0.05)	CH_2Cl_2	rt	19	no reaction
10	$[Pd(\eta^3\text{-allyl})(MeCN)_2](OTf)$ (0.05)	CH_2Cl_2	60	19	10[f] (95/5)
11	$[Pd(\eta^3\text{-allyl})(MeCN)_2](BF_4)$ (0.05)	CH_2Cl_2	60	19	46 (94/6)

[a]Experiments conducted with c = 0.1 M. Reactions at elevated temperatures where run in a sealed tube. ms = molecular sieves; Cy = c-C_6H_{11}; dppp = 1,3-bis(diphenylphosphino)propane. [b]Isolated yield after column chromatography. [c]Determined by ^1H NMR spectroscopy of the purified product. [d]Attempts to perform the reaction at 0 °C led to very low conversion rates, and a reduced solubility of the catalyst was noticed. [e]**4**, product of an oxy-Cope-rearrangement, was detected. [f]Determined by ^1H NMR spectroscopy of the crude reaction mixture. [g]Ratio: (**2a**/**3a**/**4**).

dx.doi.org/10.1021/jo3004088 | J. Org. Chem. XXXX, XXX, XXX−XXX

formation of a putative $(CH_3CN)_3Pd^{II}$–H species from $[Pd(MeCN)_4](BF_4)_2$ (Scheme 2). Regioselective coordination

Scheme 2. Conceptual Catalytic Cycle for the Cycloisomerization by a Hydropalladation/Carbopalladation/β-Hydride Elimination (HCHe) Sequence[a]

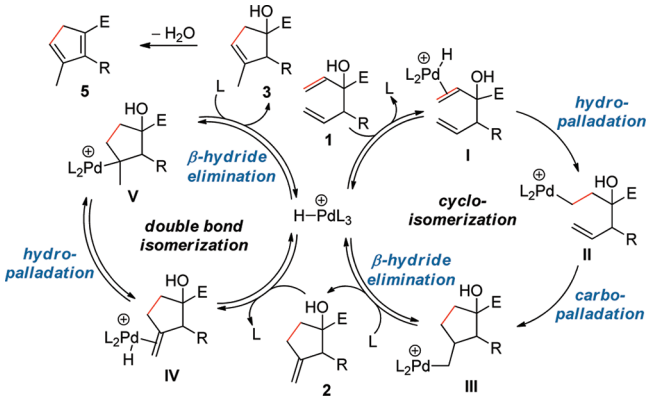

[a]Formation of the experimentally observed monomers **2**, **3** and the elimination product **5**. E = CO_2i-Pr, L = CH_3CN.

of the cationic $(CH_3CN)_3Pd^{II}$–H catalyst to the allylic double bond of **1** then delivers the $(CH_3CN)_2Pd^{II}$-π-complex **I** and subsequent hydropalladation provides the $(CH_3CN)_2Pd^{II}$-σ-alkyl-complex **II**. Ensuing 5-*exo*-*trig* carbopalladation of the homoallylic double affords the $(CH_3CN)_2Pd^{II}$-σ-cycloalkyl-intermediate **III**, which undergoes β-hydride elimination to deliver the experimentally observed methylene cyclopentane **2**; double bond isomerization and elimination (vide infra) are initiated by π-complex formation (**IV**) and subsequent hydropalladation of the exocyclic double bond of **2** to deliver the $(CH_3CN)_2Pd^{II}$-σ-complex **V**; ensuing β-hydride elimination then provides methyl cyclopentene **3**. In terms of $\Delta\Delta G°$, DFT calculations[27] predict **3** to be significantly more stable (−3.8 kcal/mol) than **2**; consequently, we expect a build-up of **3** (and **5**) on the expense of **2** as the reaction proceeds under the conditions of the cycloisomerization.

Kinetic Experiments. In order to collect evidence in support of the proposed catalytic cycle (Scheme 2), we monitored the course of the cycloisomerization by in situ ^{1}H NMR spectroscopy (Figure 1). Using the 1,5-hexadiene (±)-*syn*-**1b**, we first studied the rate and selectivity of different Pd^{II}-based precatalysts in the formation of methylene cyclopentane **2b** in $CDCl_3$ at 40 °C (Figure 1A). In accordance with our qualitative experimental observations, $[Pd(MeCN)_4](BF_4)_2$ stood out as most reactive precatalyst. In the event, a maximum build-up of **2b** (51%) was achieved after 45 min. The subsequent consumption of **2b** can be related to the formation of **3b** by double bond isomerization or **5b** by elimination. The addition of PCy_3 (0.05 equiv) clearly decelerates the rate of formation of **2b** and the build-up of **2b** levels at 46% after 18.5 h. The performance of precatalysts of the type $Pd(\eta^3\text{-allyl})(MeCN)_2](X)$ depends on the nature of the counterion X. For X = BF_4, 55% of **2b** were detected after 40 h, whereas for X = OTf, only 32% **2b** were formed within the duration of the experiment (88 h). The S-shape of the kinetic profile depicted in Figure 1A indicates a precatalyst-dependent induction period for the formation of the actual cycloisomerization catalyst, supposedly a L_nPd–H species, and the most electrophilic precatalyst, the "bis-cationic" $[Pd(MeCN)_4](BF_4)_2$ complex requires the shortest induction period.[28] We continued the kinetic profiling by monitoring the entire product genesis from (±)-*syn*-**1b** in the presence of $[Pd(MeCN)_4](BF_4)_2$ (0.05 equiv) in $CDCl_3$ at 27 °C (Figure 1B). Formation of the cyclopentane **2b** is dominating from the outset and levels at 60% after 10 h. Upon its formation, **2b** is steadily consumed because of double bond isomerization to **3b**, which in turn, is subsequently converted to cyclopentadiene **5b** by formal elimination of water. Notably, build-up of the previously unnoticed dimer **6b**[29,30] was detected, and, when considering that the connection of the diene fragment to the cyclopentane ring occurs at C2′, it is evident that the genesis of **6b** requires a different and competing cycloisomerization pathway, which is initiated by hydropalladation of the homoallylic double bond. Following the maximum build-up (19%, 8 h), **6b** is consumed by a downstream bond building to products that were untraceable in this experiment.

Kinetic profiling of the solvent-dependence of the product genesis led to further insight into the unprecedented dimerization. Monitoring product formation for **1b** in the presence of $[Pd(MeCN)_4](BF_4)_2$ (0.05 equiv) in acetone-d_6 (27 °C, 20 h) (Figure 1C, 1D) indicates faster consumption than in $CDCl_3$ and decreased initial selectivity in favor of **2b** (44% maximum build-up after 8 h). As it was the case in $CDCl_3$, double bond isomerization to **3b** and subsequent elimination to **5b** are notable. Furthermore, the competing dimerization is more pronounced, which leads to a significant build-up of **6b** (33% after 6 h). Monocyclic dimer **6b** is than consumed to afford the dimer **7b**;[31] this bond forming cascade is operative even after full consumption of **1b**, indicating the formation of **7b** from **1b** via **6b**.

Generalized Product Distribution in 1,5-Hexadiene Cycloisomerizations. The interplay and dependence of the various bond-forming events under the cycloisomerization conditions is subtle, and we expected the substrate structure as a key determinant. In order to validate that the established bond forming cascades are general, different 1,5-hexadienes were synthesized and subjected to the conditions of the cycloisomerization (Table 2). In line with our previous experiments, the monocycloisomerized dimer **6c** (22%) resulted from the cycloisomerization of (±)-**1c**[20] (Table 2, entry 1), and the dimers **6d** and **7d** were obtained from the cycloisomerization of (±)-**1d** (Table 2, entry 2). Notably, the cycloisomerization of (±)-**1e** delivered the elusive regioisomeric methylene cyclopentane (±)-**2e′**, although in very minute amounts, along with the dimer **7e** as a mixture of diastereomers (Table 2, entry 3); from this mixture, the S_2 symmetric diastereomer **7e** could be crystallized, and crystal structure analysis corroborated our structural assignment.[32] In accordance with a Thorpe–Ingold effect,[33] the cycloisomerization of (±)-**1f** proceeded extremely fast (complete consumption of **1f** in less than 30 min) and afforded the expected mixture monomers and dimers (Table 2, entry 4); the S_2 symmetric dimer **7f** was subjected to X-ray crystallography.[34]

Conceptual Catalytic Cycle for Dimer Formation. Considering the experimental evidence discussed above, a feasible qualitative catalytic cycle for the formation of the dimers **6**, **7** and the monomer **2′** from hexadiene **1** can be proclaimed (Scheme 3). We propose a bond-forming cascade initiated by an interrupted cycloisomerization of **1**, which proceeds via the hydropalladation product **VI** to the carbopalladation product **VII**, which resists β-hydride elimination. As an alternative for β-hydride elimination, formation of the π-complex **VIII** can be

dx.doi.org/10.1021/jo3004088 | J. Org. Chem. XXXX, XXX, XXX–XXX

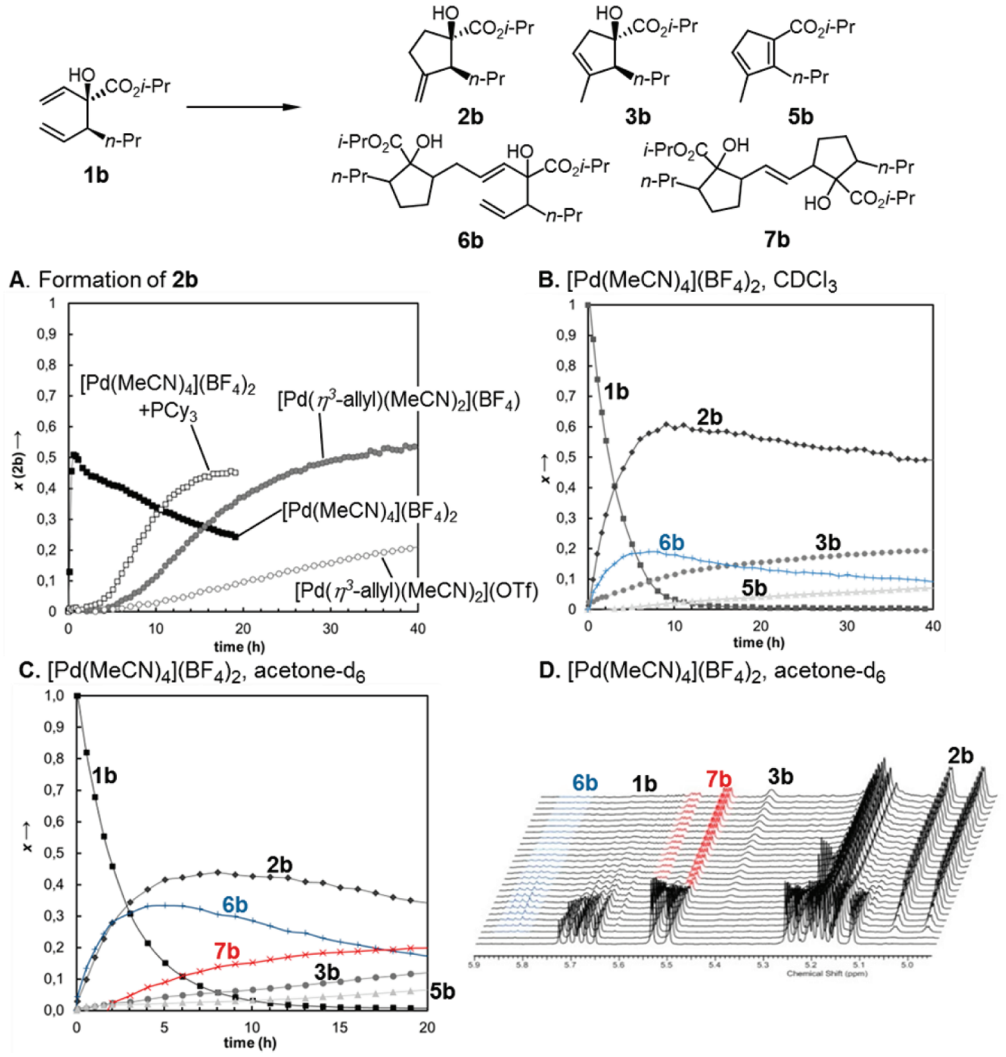

Figure 1. (A) Screening (^{1}H NMR, $CDCl_3$, 40 °C) of precatalysts (0.05 equiv) for the cycloisomerization of **1b** to **2b**. (B) Kinetic profile (^{1}H NMR, $CDCl_3$, 27 °C) for the cycloisomerization of **1b** with $[Pd(MeCN)_4](BF_4)_2$ (0.05 equiv). (C) ^{1}H NMR kinetic profile (^{1}H NMR, acetone-d_6, 27 °C) for the cycloisomerization of **1b** with $[Pd(MeCN)_4](BF_4)_2$ (0.05 equiv). (D) Section of the ^{1}H NMR array. All experiments were performed using a Shigemi NMR tube and with c = 0.1 M.

assumed, and subsequent intermolecular carbopalladation to afford **IX** redirects the initial cycloisomerization toward dimerization. The dimerization process is continued by β-hydride elimination to afford the π-complex **X** and the experimentally observed monocyclic dimer **6**. Subsequent hydropalladation of **6** at the terminal double bond delivers the Pd^{II}-σ-complex **XI**, which undergoes an intramolecular carbopalladation and subsequent β-hydride elimination to conclude the catalytic cycle and to provide the experimentally observed bicyclic dimer **7**.

Interrupted and Redirected Cycloisomerization. According to our mechanistic proposal, the β-hydride elimination from the Pd(II)-σ-cycloalkyl-intermediate **III** is essential to conclude the simple catalytic cycle of the HCHe cascade (Scheme 2). Consequently, it should be possible to telescope the cycloisomerization pathway, which was initiated by hydropalladation of the allylic double bond, toward dimerization by preventing β-hydride elimination; in this regard, replacement of the β-hydride by a non-hydrogen atom substituent should enforce dimerization by Heck reaction (Scheme 4). In order to experimentally validate the proposal of an interrupted and redirected cycloisomerization (Scheme 3), the tailor-made 1,5-hexadiene (±)-**1g** was subjected to $[Pd(MeCN)_4](BF_4)_2$ (0.05 equiv) in CH_2Cl_2 at room temperature for 72 h and delivered the expected monocycloisomerized dimer (±)-**8** as a mixture of diastereomers.

COMPUTATIONAL CHEMISTRY

DFT Calculations. Computational studies were initiated with the intent to support and to refine the conceptual catalytic cycle for the cycloisomerization. In particular, we sought to understand how the regioselectivity of the initial hydropalladation (allylic versus homoallylic double bond) predetermines the final product formation (monomers versus dimers). According to the conceptual catalytic cycles (Schemes 2 and 4), the overall cycloisomerization process consists of a hydropalladation/carbopalladation/β-hydride elimination (HCHe) sequence; accordingly, the results of the DFT calculations will be presented cumulatively.

Computational Details. All calculations where performed with the Gaussian03[35] suite of programs at DFT level with the B3LYP[36] functional. Geometry optimizations were performed without restrictions and default convergence criteria with the LACVP(d)[37] basis set in the gas phase at 298.15 K. The basis set consists of the standard 6-31G(d) basis set for the atoms (H, C, N, O) and the LANL2DZ basis set, which contains an effective core potential (ECP)

dx.doi.org/10.1021/jo3004088 | J. Org. Chem. XXXX, XXX, XXX−XXX

Table 2. Product Distribution in the Cycloisomerization of Substituted 1,5-Hexadienes 1c–f[a]

entry	1,5-hexadiene	product	yield (%) (**2**/**3**/**6**/**7**)[b]
1	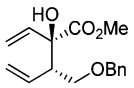 (±)-**1c**	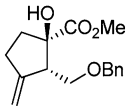 (±)-**2c** 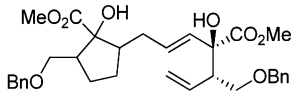 (±)-**6c**	44 (45/0/55/0)
2	 (±)-**1d**	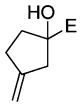 (±)-**2d** 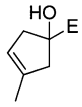 (±)-**3d** 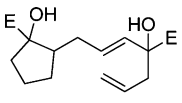 (±)-**6d** 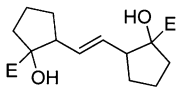 **7d**	48 (29/4/49/18)
3	 (±)-**1e**	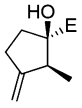 (±)-**2e** 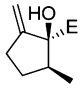 (±)-**2e'** 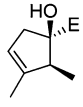 (±)-**3e** 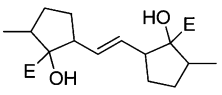 **7e**	48 (14/3/6/0/77)[d]
4[c]	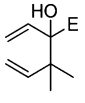 (±)-**1f**	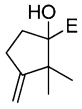 (±)-**2f** 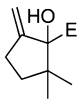 (±)-**2f'** 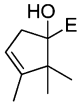 (±)-**3f** 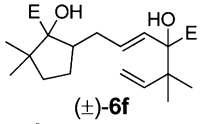 (±)-**6f** 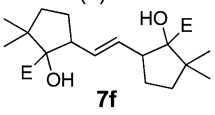 **7f**	79 (24/8/3/39/26)[d]

[a]Conditions: $[Pd(MeCN)_4](BF_4)_2$ (0.05 equiv), CH_2Cl_2 (c = 0.1 M), rt, 3–23 h. E = CO_2i-Pr. [b]Determined by ^1H NMR spectroscopy of the purified product mixture. [c]Addition of PCy_3 (0.05 equiv) in order to induce a more manageable rate of conversion. [d]Ratio: (**2**/**2′**/**3**/**6**/**7**).

Scheme 3. Conceptual Catalytic Cycle for the Interrupted and Redirected Cycloisomerization[a]

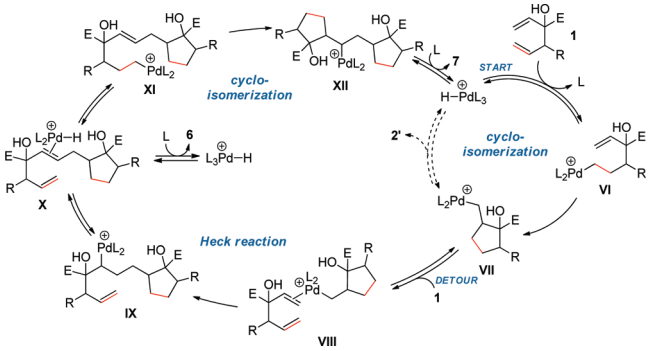

[a]Formation of the experimentally observed dimers **6**, **7** and the monomer **2′**. E = CO_2i-Pr, L = CH_3CN.

Scheme 4. Interrupted and Redirected Cycloisomerization: Enforced Dimerization of 1,5-Hexadiene (±)-1g

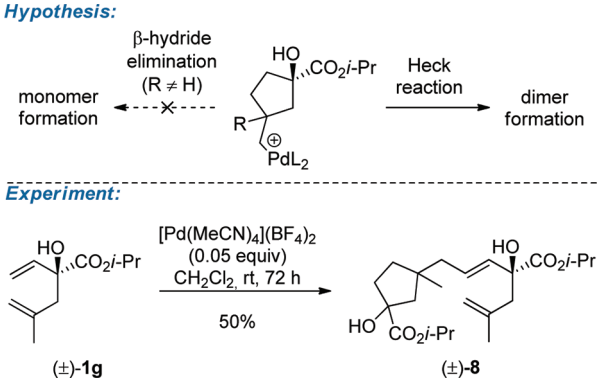

with a split valence (double-ζ) basis set for Pd. For more accurate energy values, all optimized structures were reoptimized with the def2-SVP[38] (double-ζ) basis set for Pd and the 6-31++G(d,p) basis set for the lighter atoms, as implemented in Gaussian03. Harmonic frequencies were calculated at the same level of theory to identify the nature of stationary points as minima (zero imaginary frequencies in the Hessian matrix) or transition states (one imaginary frequency; animation of the vibrational mode verified the reaction coordinate) and to obtain zero-point energy corrections (ZPC). In addition, relevant transitions states were verified by IRC-calculations. On the optimized geometries, single-point calculations were performed with the def2-TZVP[38,39] (triple-ζ) basis set, defined by Weigend and Ahlrichs. The obtained results showed no significant variations of the previously observed trends. To reduce computational cost, we employed a model system for our calculations with the following simplifications: (i) the isopropyl ester group was replaced by a methyl ester group; (ii) the substituent at C4 was reduced to a methyl group; and (iii) the catalytical active "Pd–H"-complex was expressed by $[PdH(MeCN)_3]^+$ with square planar geometry. Energies reported in the text section correspond to the relative electronic energies after zero-point energy correction (ΔE+ZPC). In Figures 2–7, Gibbs free energies (ΔG) are included in parentheses.

Regioselectivity of the Hydropalladation. The cycloisomerization-triggering hydropalladation of the allylic or the homoallylic double bond of the 1,5-hexadienes **1** constitutes the branching point for subsequent product formation by the HCHe sequence (Scheme 5). Therefore, we embarked on our computational endeavor by modeling the competing hydropalladation pathways.

After a careful examination of various $(CH_3CN)_2Pd$·1,5-hexadiene π-complexes, we identified the π-complex **M1** as most stable *bis*(acetonitrile) complex and normalized its energy to zero. Starting from **M1**, our gas phase calculations predict that the hydropalladation of the allylic double bond **TS(M1–M2)** proceeds almost barrierless and provides the more stable (−4.2 kcal/mol) β-agostic complex **M2** (Figure 2). Notably,

dx.doi.org/10.1021/jo3004088 | J. Org. Chem. XXXX, XXX, XXX–XXX

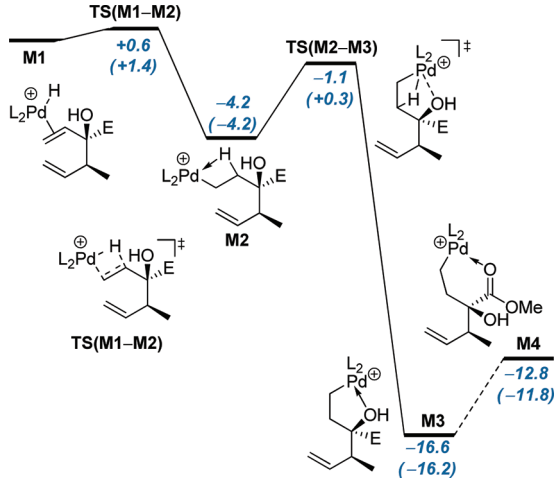

Figure 2. B3LYP/(Def2-TZVP + 6-31++G(d,p)) calculated ΔE (ΔG) in kcal/mol for the allylic hydropalladation; all energies relative to **M1**. E = CO_2Me, L = CH_3CN.

Scheme 5. Allylic vs. Homoallylic Hydropalladation[a]

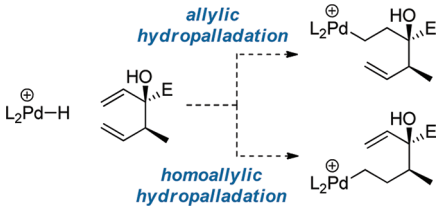

[a]E = CO_2Me, L = CH_3CN.

our initial hydropalladation scenario (Scheme 5) is expanded by the localization of the five-membered Pd^{II}-hydroxo-chelate complex **M3** as well as the six-membered Pd^{II}-carbonyl-chelate complex **M4**.[17,40] Considering the low barrier (3.1 kcal/mol) for the formation of **M3** from **M2** and its stability relative to **M2** (−12.4 kcal/mol) and **M4** (−3.8 kcal/mol), we consider **M3** as pivotal intermediate on the reaction coordinate.

The competing hydropalladation of the homoallylic double bond was modeled next (Figure 3). In the event, formation of the less stable

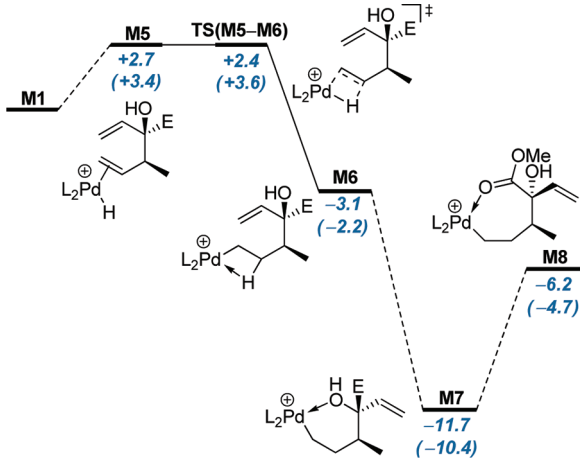

Figure 3. B3LYP/(Def2-TZVP + 6-31++G(d,p)) calculated ΔE (ΔG) in kcal/mol for the homoallylic hydropalladation; all energies relative to **M1**. E = CO_2Me, L = CH_3CN.

(+2.6 kcal/mol) π-complex **M5** from **M1** is required to open a barrierless exoenergetic (−3.2 kcal/mol) hydropalladation pathway to the β-agostic σ-complex **M6**. Our search for stable chelate complexes led to the localization of the six-membered Pd^{II}-hydroxo-chelate complex **M7** and the seven-membered Pd^{II}-carbonyl complex **M8**. No attempt was made to model the multiple conformational changes required for the exoenergetic formation of **M7** (−11.7 kcal/mol) from **M6**. Nevertheless, we assume the kinetic accessibility of **M7** and consider **M7** as inevitable intermediate on the (interrupted) HCHe pathway.

Overall, our analysis of the regioselectivity of the hydropalladation suggests a rapid and irreversible process, which affords the Pd^{II}-hydroxo-chelate complexes **M3** and **M7**. In accordance with the experimentally observed product ratios, the calculations do not rule out a competition between the allylic and homoallylic hydropalladation pathways.

Carbopalladation and β-Hydride Elimination. Beyond the hydropalladation branching point to the constitutional isomers **M3** and **M7**, modeling the HCHe pathway requires separate treatment of the fate of the two pivotal intermediates **M3** and **M7**. Furthermore, for both intermediates, the 5-*exo-trig* carbopalladation is a diastereoface-differentiating elementary reaction. The results of the computational analysis of the *Re*- and *Si*-face 5-*exo-trig* carbopalladation of the homoallylic double bond in **M3** will be discussed first.

The 5-*exo-trig* carbopalladation of the homoallylic double in **M3** is, as schematized in Scheme 6, a branching point to diastereomeric

Scheme 6. Principle Branching Point within the Hydropalladation/Carbopalladation/β-Hydride Elimination (HCHe) Process[a]

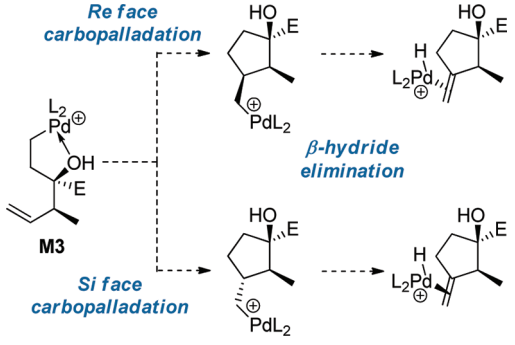

[a]*Re*- and *Si*-Face carbopalladation of the homoallylic double bond. E = CO_2Me, L = CH_3CN.

cyclopentylmethyl-Pd^{II}-σ-complexes, which by way of β-hydride elimination, are converted to diastereomeric hydrido-Pd^{II}-π-complexes containing the identical methylene cyclopentane ligand. Accordingly, whether or not the 5-*exo-trig* carbopalladation is effectively diastereoface-differentiating, the existence of a principle branching point is inconsequential, at least with respect to the expectable product spectrum. However, and possibly unexpectedly, our computational analysis outlined below suggests a more sophisticated course in which kinetics prevent the formation of a thermodynamically dominant, possibly HCHe-interrupting Pd^{II}-hydroxo-chelate complex.

The computationally predicted pathway required for and resulting from the 5-*exo-trig* *Si*-face carbopalladation of **M3** is depicted in Figure 4. The carbopalladation event requires the formation of the π-complex **M9** from the Pd^{II}-hydroxo-chelate complex **M3**. The calculations predict an endoenergetic intramolecular ligand exchange process (+4.7 kcal/mol) with a significant barrier (12.1 kcal/mol). Notably, **M9** appears to be a 1,3-allylic strain-minimized conformer. Subsequent 5-*exo-trig* carbopalladation proceeds from **M9** via the *cis*-bicyclo[3.2.0]heptane-like transition-state structure **TS(M9−M10)** with significant barrier (+11.5 kcal/mol) to deliver exoenergetically (−1.2 kcal) the γ-agostic complex **M10**. The predicted γ-agostic complex **M10** is separated from the significantly more stable (−8.5 kcal/mol) β-agostic complex **M11** by a rather minute barrier (3.0 kcal/mol). Our search for chelate complexes of the carbopalladation product led to the localization of the Pd^{II}-carbonyl-σ-complex **M12** (−21.2 kcal/mol relative to **M1**), which is nearly isoenergetic to the β-agostic complex **M11** (−21.6 kcal/mol relative to **M1**). The concluding β-hydride

dx.doi.org/10.1021/jo3004088 | J. Org. Chem. XXXX, XXX, XXX−XXX

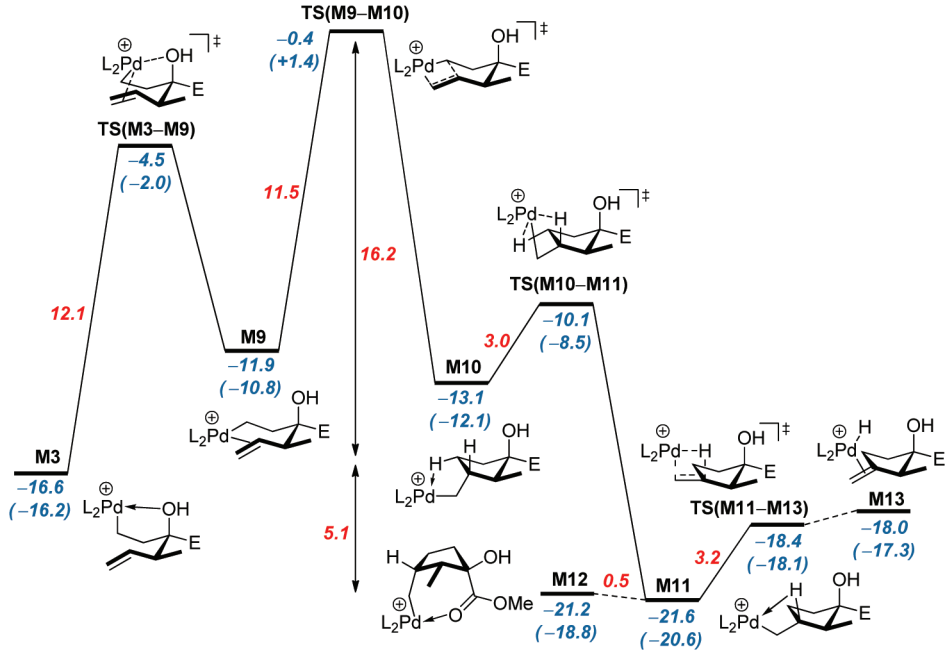

Figure 4. B3LYP/(Def2-TZVP + 6-31++G(d,p)) calculated ΔE (ΔG) in kcal/mol for the *Si*-face 5-*exo*-*trig* carbopalladation of the homoallylic double bond, and subsequent β-hydride elimination; all energies relative to **M1**. E = CO_2Me, L = CH_3CN.

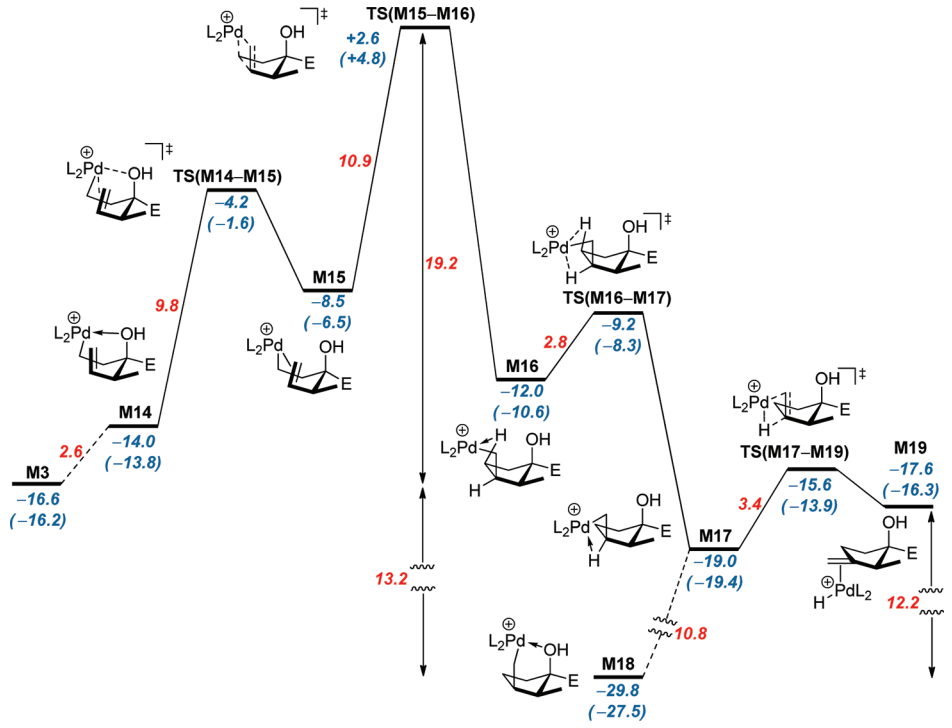

Figure 5. B3LYP/(Def2-TZVP + 6-31++G(d,p)) calculated ΔE (ΔG) in kcal/mol for the *Re*-face 5-*exo*-*trig* carbopalladation of the homoallylic double bond, and subsequent β-hydride elimination; all energies relative to **M1**. E = CO_2Me, L = CH_3CN.

elimination process proceeds endoenergetically and with a low barrier from **M11** via **TS(M11−M13)** to the hydrido-Pd^{II}-π-complex **M13**.[41]

Overall, our modeled pathway for a sequential 5-*exo*-*trig* carbopalladation/β-hydride elimination from **M3** to **M13** is well passable with an energetic span of 16.2 kcal/mol between the rate determining intermediate **M3** and the rate-determining transition-state **TS(M9−M10)**. The carbopalladation event is slow and irreversible, whereas the concluding β-hydride elimination is fast and reversible. The nonproductive Pd^{II}-carbonyl-σ-chelate complex **M12** is energetically accessible but does not represent an interrupting resting state for the HCHe process.

The course of competing 5-*exo*-*trig* *Re*-face carbopalladation of the homoallylic double bond is depicted in Figure 5. The carbopalladation elementary reaction requires the endoenergetic formation (+8.1 kcal/mol) of the π-complex **M15** from the Pd^{II}-hydroxo-chelate complex **M3**. Notably, **M15** could be destabilized by complexation-enforced 1,3-allylic strain. In quite close analogy to the processing of **M9** (Figure 4), the carbopalladation of **M15** proceeds with a manageable barrier to provide, exoenergetically (−3.5 kcal/mol), the γ-agostic complex **M16**, which is separated from the more stable β-agostic complex **M17** by insignificant barrier (2.8 kcal/mol). The marked difference between

dx.doi.org/10.1021/jo3004088 | J. Org. Chem. XXXX, XXX, XXX−XXX

the *Re*- and the *Si*-face carbopalladation process surfaced once we located the hydroxo-chelate complex **M18**. Whereas the Pd^{II}-carbonyl-chelate complex **M12** is isoenergetic to the β-hydride complex **M11** (Figure 4), the corresponding six-membered Pd^{II}-hydroxo-chelate complex **M18** represents a thermodynamic resting state, which renders the concluding β-hydride elimination of the HCHe process prohibitively endoenergetic (+14.2 kcal/mol).

Altogether, our calculations predict that the *Re*-face carbopalladation of the homoallylic double would inevitably lead to the formation of the Pd^{II}-hydroxo-chelate complex **M18**, a thermodynamic resting state off the HCHe pathway, which would interrupt and, possibly, redirect the HCHe pathway toward dimerization. Experimentally, however, we have not yet been able to isolate noticeable amounts of dimers resulting from a Heck-type reaction of **M18**. Consistently, our calculations predict a kinetic preference for the *Si*-face over the *Re*-face carbopalladation process (**TS(M9−M10)** versus **TS(M15−M16)**, $\Delta\Delta E^{\ddagger}$ = 3 kcal/mol) and, therefore, in favor of the uninterrupted HCHe pathway.

So far, we revealed that in accordance with the experimentally observed formation of methylene cyclopentanes **2a−f** by the cycloisomerization of 1,5-hexadienes **1a−f**, modeling the HCHe process initiated at the allylic double bond suggests a passable pathway from the π-complex **M1** via **M3** and **M11** to **M13**. Having already calculated the hydropalladation pathway from **M1** to **M7** (Figure 5), we focused on the branching pathways arising from the *Re*- or *Si*-face 5-*exo*-*trig* carbopalladation of the allylic double bond of **M7** (Scheme 7).

Scheme 7. Principle Branching Point within the Hydropalladation/Carbopalladation/β-Hydride Elimination (HCHe) Process[a]

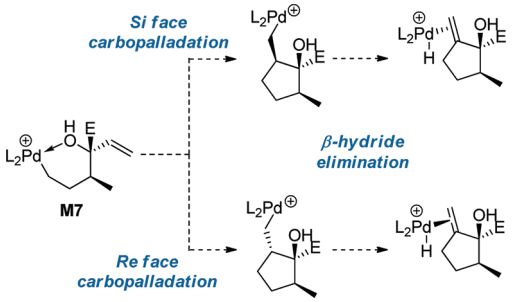

[a]*Re*- and *Si*-Face carbopalladation of the allylic double bond. E = CO_2Me, L = CH_3CN.

Intrigued by the unexpected experimental observation that hydropalladation of the homoallylic double bond triggers formation of dimers rather than monomeric methylene cyclopentanes (Scheme 4), hence disapproving the expected (Scheme 7), we sought mechanistic insights by computational chemistry.

The computed pathway for the *Re*-face 5-*exo*-*trig* carbopalladation of the allylic double bond will be discussed first (Figure 6). Starting from the Pd^{II}-hydroxo-chelate complex **M7** and with the intermediacy of the conformer **M20**, we propose a rapid formation of the Pd^{II}-olefin-chelate π-complex **M21**. The elementary carbopalladation process proceeds slightly endonergetically (+1.7 kcal/mol from **M7**) and with a conquerable barrier (15.0 kcal/mol) to deliver the γ-agostic complex **M22**. In line with our previous computations, the γ-agostic complex is separated from the significantly more stable β-agostic complex **M23** (−8.4 kcal/mol) only by a low-lying transition state (+3.1 kcal/mol). Mindful of the importance of Pd^{II}-O-donor-chelate complexes in shaping the energy landscape, we scanned for and localized the off-pathway chelate complexes **M24** (−5.3 kcal/mol relative to **M23**) and **M25** (−6.6 kcal/mol relative to **M23**), both markedly more stable than the on-pathway complex **M23**. Consequently, the stability and the proposed kinetic accessibility of **M25** would interrupt the HCHe process by rendering the terminating β-hydride elimination to **M26** unfavorable (+10.7 kcal/mol).

Looking back at our conceptual catalytic cycle for dimer formation (Scheme 4), the then proposed resistance of the conceptual intermediate **VII** toward β-hydride elimination can now be understood as a consequence of the formation of off-pathway Pd^{II}-O-donor-chelate σ-complexes, **M24** or **M25** (Figure 6), whose thermodynamic stability interrupts the HCHe catalytic cycle and redirects the bond forming cascade toward dimer formation. This mechanistic origin of the experimentally observed dimer formation is even more convincingly illustrated by the modeled pathway of the *Si*-face 5-*exo*-*trig* carbopalladation of the allylic double bond (Figure 7).

The modeled pathway initiated by the *Si*-face 5-*exo*-*trig* carbopalladation of the allylic double bond progresses from the Pd^{II}-hydroxo-chelate complex **M7** via the π-complex **M27** and the transition state **TS(M27−M28)** to provide, highly exoenergetic (−20.2 kcal/mol), the five-membered Pd^{II}-hydroxo-chelate complex **M28**; upstream agostic Pd^{II} σ-complexes could not be located. Comparing the calculated activation barriers for the competing carbopalladation pathways via **TS(M21−M22)** (+15.9 kcal/mol, Figure 6) or **TS(M27−M28)** (+12.0 kcal/mol, Figure 7) indicates a marked kinetic preference ($\Delta\Delta E^{\ddagger}$ = 3.9 kcal/mol) for the *Si*-face 5-*exo*-*trig* carbopalladation pathway depicted in Figure 7. Consequently, we consider the *Si*-face 5-*exo*-*trig* carbopalladation pathway as kinetically dominant. Hitherto, the transition state of the carbopalladation elementary reaction represented the rate-determining transition state (Figures 4−6). The predicted stability of the Pd^{II}-hydroxo-chelate complex **M28** now deeply changes the appearance of the energy landscape (Figure 7): **M28** at −31.9 kcal/mol and the transition state for β-hydride elimination **TS(M30−M31)** at −11.2 kcal/mol are now the energetic span-defining states, and the resulting effective barrier (+20.7 kcal/mol) is much higher than before. More significantly, the Pd^{II}-hydroxo-chelate complex **M28** represents a prototypic off-pathway resting state that resists β-hydride elimination and serves as redirecting point to the experimentally noticed dimer formation. Notably, the predicted all-*cis* relative configuration of **M28** matches the relative configuration of the S_2 symmetric dimers **7e** and **7f** that were characterized by X-ray crystallography.

CONCLUSION

Using the commercially available precatalyst $[Pd(MeCN)_4](BF_4)_2$, highly functionalized 1,5-hexadienes have been converted to valuable methylene cyclopentane building blocks. This low-temperature cycloisomerization is fast and effective; double bond isomerization and elimination can be minimized by optimizing the reaction conditions, but its efficiency is clearly affected by the propensity for dimer formation. Catalyst optimization has so far met with limited success; for instance, the presence of phosphine ligands is detrimental to the activity of the catalyst. In situ NMR studies delivered valuable insights into the product formation process, and X-ray crystallography helped to assign the constitution and configuration of dimeric products.

To summarize the computational part of this study, the predicted essentials of the competing open and interrupted hydropalladation/carbopalladation/β-hydride elimination (HCHe) processes are depicted in Figure 8. The site-selectivity of the initiating hydropalladation determines the chemoselectivity (monomer versus dimer formation). Hydropalladation at the allylic double bond initiates an intact HCHe cycle, which proceeds from **M1** by a fast and irreversible hydropalladation to deliver the Pd^{II}-hydroxo-chelate complex **M3**, which is converted by the rate-limiting and irreversible carbopalladation to the β-agostic methylcyclopentane Pd^{II} σ-complex **M11**. Fast and reversible β-hydride elimination then affords the π-complex **M13**, and the slightly exoenergetic ligand exchange to **M1** completes the HCHe cycle. The hydropalladation

dx.doi.org/10.1021/jo3004088 | J. Org. Chem. XXXX, XXX, XXX−XXX

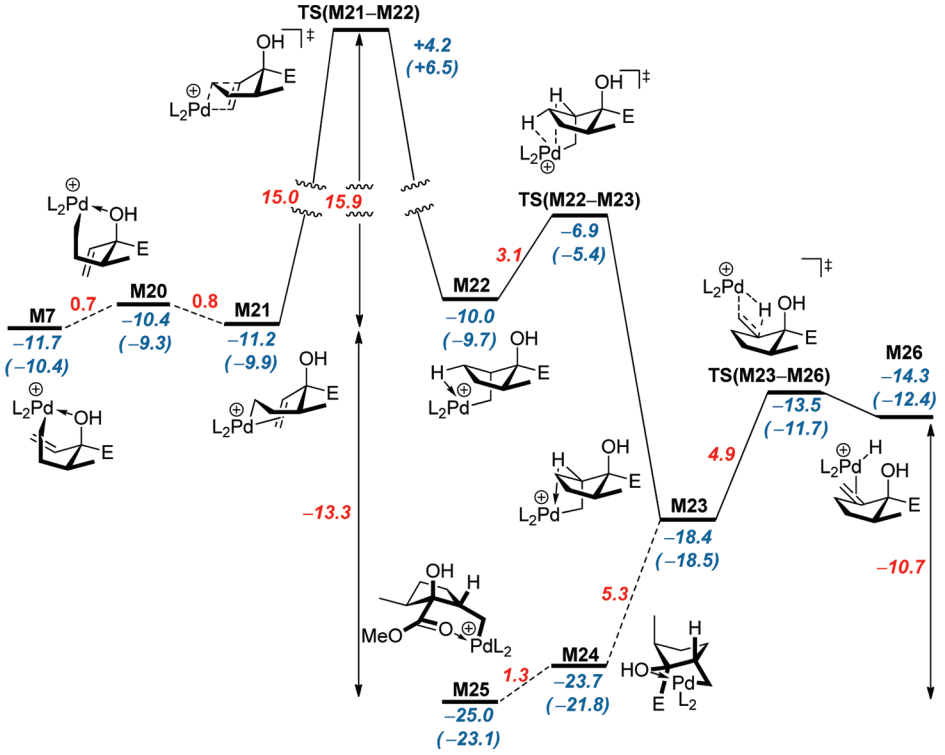

Figure 6. B3LYP/(Def2-TZVP + 6-31++G(d,p)) calculated ΔE (ΔG) in kcal/mol for the *Re*-face 5-*exo*-*trig* carbopalladation of the allylic double bond, and subsequent β-hydride elimination; all energies relative to **M1**. E = CO_2Me, L = CH_3CN.

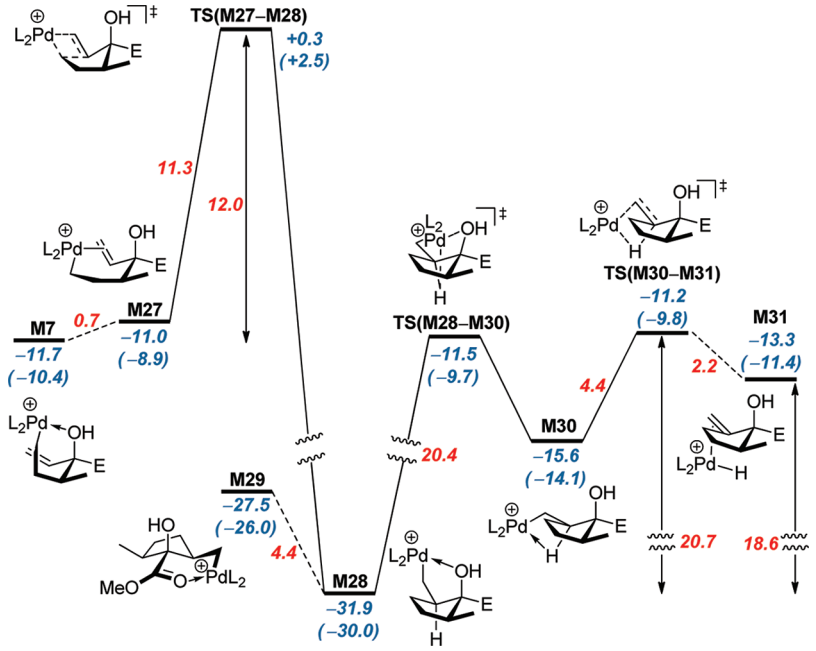

Figure 7. B3LYP/(Def2-TZVP + 6-31++G(d,p)) calculated ΔE (ΔG) in kcal/mol for the *Si*-face 5-*exo*-*trig* carbopalladation of the allylic double bond, and subsequent β-hydride elimination; all energies relative to **M1**. E = CO_2Me, L = CH_3CN.

of the homoallylic double bond is kinetically competitive and initiates an interrupted and redirected HCHe cycle, which proceeds from **M5** by a fast and irreversible hydropalladation to the Pd^{II}-hydroxo-chelate complex **M7**, which is converted by carbopalladation to afford the off-pathway Pd^{II}-hydroxo-chelate complex **M28**, whose intermediacy renders the β-hydride elimination to **M31** prohibitively endoenergetic. We propose that the Pd^{II}-hydroxo-chelate complex **M28** represents the interrupting off-pathway intermediate, which redirects the HCHe pathway toward dimer formation.

We believe that as soon as the complexes **M1** or **M5** are formed, the hydropalladation occurs rapidly and irreversibly; the site-selectivity and, therefore, chemoselectivity originates from the capability of the catalyst to differentiate between the heterotopic double bonds. The current catalyst system is moderately successful in this regard, but our computations

dx.doi.org/10.1021/jo3004088 | J. Org. Chem. XXXX, XXX, XXX–XXX

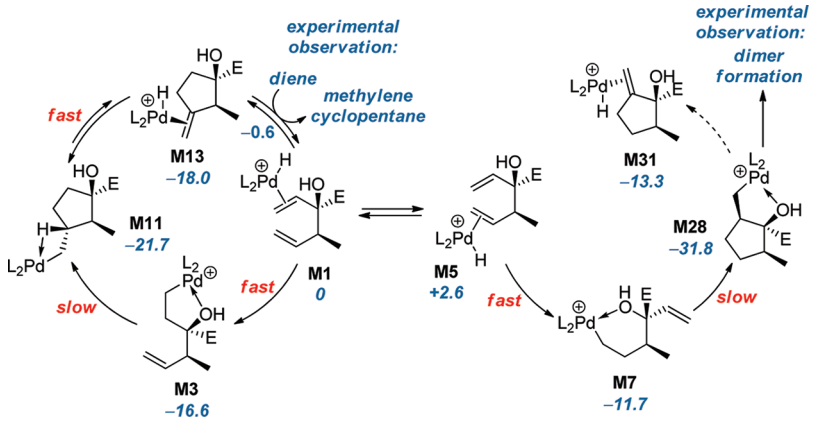

Figure 8. Computationally predicted essentials of the competition between the open and the interrupted hydropalladation/carbopalladation/β-hydride elimination (HCHe) processes. E = CO_2Me, L = CH_3CN.

provide no insights into factors that determine the site-differentiation. Future experimental work will be directed toward the development of more selective, site-differentiating hydropalladation catalysts that are competent to carry an open HCHe cycle without surrendering the characteristics of the substrate structure. Future efforts in computational chemistry will be directed toward an understanding of the factors that should promote the site-differentiating hydropalladation as well as the mechanistic details of the dimer formation.

EXPERIMENTAL SECTION

General Procedure for the Dienolate [2,3]-Wittig Rearrangement.[42] A cooled (−85 °C) solution of LDA [prepared in situ from (i-Pr)$_2$NH (1.2−1.3 equiv) and n-BuLi (1.1−1.4 equiv of n-BuLi, titrated employing diphenylacetic acid as indicator[43])] in dry THF (2 mL/mmol) was treated dropwise with a cooled (−85 °C) solution of the allyl vinyl ether (1 equiv, mixture of double bond isomers) in dry THF (3 mL/mmol). The resulting light yellow solution was stirred for a period of 10−30 min (−85 → approximately −70 °C). The dry ice bath was then replaced by a cooling bath, and the reaction mixture was stirred at 0 °C until TLC indicated complete conversion of the starting material (10 min−1 h). In most cases, successful reaction was accompanied by a color change from light yellow to orange/red. The solution was subsequently diluted by the addition of aqueous saturated NH_4Cl solution at 0 °C and warmed to room temperature. The aqueous layer was extracted with CH_2Cl_2 (3×). The combined organic phases were dried ($MgSO_4$) and concentrated under reduced pressure. Purification by flash chromatography (cyclohexane/ethyl acetate) afforded the corresponding 1,5-hexadiene (±)-**1** as a mixture of diastereomers.

1,5-Hexadiene (±)-**1d**. According to the general procedure for the [2,3]-Wittig rearrangement, the reaction of allyl vinyl ether **9**[44] (1.8 g, 10 mmol) with (i-Pr)$_2$NH (1.8 mL, 13 mmol, 1.3 equiv) and n-BuLi (5.1 mL, 12 mmol, 1.2 equiv, 2.35 M in hexanes) in THF (20 + 30 mL) at −85 → −70 °C (30 min) and 0 °C (1 h) provided 1,5-hexadiene (±)-**1d** (1.44 g, 12.7 mmol, 78%) after flash chromatography (cyclohexane/ethyl acetate 100/1): R_f 0.57 (cyclohexane/ethyl acetate 5/1); ^{1}H NMR ($CDCl_3$, 500 MHz, δ) 1.27 (d, J = 6.0 Hz, 3H), 1.28 (d, J = 6.1 Hz, 3H), 2.43 (dd, J = 14.0, 6.5 Hz, 1H), 2.58 (dd, J = 14.0, 7.9 Hz, 1H), 3.34 (s, 1H), 5.06 (spt, J = 6.3 Hz, 1H), 5.11 (s, 1H), 5.14 (d, J = 5.0 Hz, 1H), 5.19 (dd, J = 10.6, 1.2 Hz, 1H), 5.50 (dd, J = 17.1, 1.2 Hz, 1H), 5.72−5.83 (m, 1H), 5.98 (dd, J = 17.1, 10.5 Hz, 1H); ^{13}C NMR ($CDCl_3$, 126 MHz, δ) 21.8 (CH_3), 21.9 (CH_3), 43.6 (CH_2), 70.3 (CH), 77.1 (C), 115.3 (CH_2), 119.1 (CH_2), 132.2 (CH), 138.6 (CH), 174.1 (C); IR (cm^{-1}) 3520(br m) (ν OH), 2985(m), 2960(s), 2940(w), 1725(s) (ν C═O), 1645(m) (ν C═C), 1470(w), 1435(w), 1375(m), 1275(m), 1225(s) (ν C−O−C ester), 1175(s), 1105(s), 995(m). Anal. Calcd. for $C_{10}H_{16}O_3$: C, 65.2; H, 8.8. Found: C, 65.1; H, 9.1; $C_{10}H_{16}O_3$, M =184.23 g/mol.

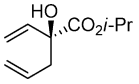

1,5-Hexadiene (±)-**1e**. According to the general procedure for the [2,3]-Wittig rearrangement, the reaction of allyl vinyl ether **10**[45] (0.99 g, 5 mmol) with (i-Pr)$_2$NH (0.84 mL, 6 mmol, 1.2 equiv) and n-BuLi (2.4 mL, 5.5 mmol, 1.1 equiv, 2.3 M in hexanes) in THF (10 mL + 15 mL) at −85 → −70 °C (10 min) and 0 °C (10 min) provided 1,5-hexadiene (±)-**1e** (0.47 g, 2.4 mmol, 48%) after flash chromatography (cyclohexane/ethyl acetate 200/1 → 50/1) as a mixture of diastereomers (*syn*/*anti* = 77/23): R_f 0.66 (cyclohexane/ethyl acetate 5/1); ^{1}H NMR ($CDCl_3$, 400 MHz, mixture of diastereomers *syn*/*anti* = 77/23, δ) 0.99 (d, J = 6.9 Hz, 3H), 1.22−1.31 (m, 6H), 2.54−2.69 (m, 1H), 3.27 (s, 0.8H^{major}), 3.31 (s, 0.2H^{minor}), 4.95−5.05 (m, 2H), 5.06−5.12 (m, 1H), 5.18 (dd, J = 10.5, 1.4 Hz, 0.2H^{minor}), 5.22 (dd, J = 10.5, 1.5 Hz, 0.8H^{major}), 5.45 (dd, J = 17.1, 1.4 Hz, 0.2H^{minor}), 5.52 (dd, J = 17.0, 1.5 Hz, 0.8H^{major}), 5.69−5.81 (m, 1H), 5.89 (dd, J = 17.0, 10.5 Hz, 0.8H^{major}), eclipsed by 5.92 (dd, J = 17.2, 10.2 Hz, 0.2H^{minor}); ^{13}C NMR ($CDCl_3$, 101 MHz, mixture of diastereomers *syn*/*anti* = 77/23, δ) 13.7/14.4 (CH_3), 21.8/21.9 (2 × CH_3), 44.8/45.1 (CH), 70.2/70.3 (CH), 79.3/79.6 (C), 115.6/116.0 (CH_2), 116.1/116.4 (CH_2), 137.8/138.2 (CH), 138.4/138.7 (CH), 174.4/174.5 (C); IR (cm^{-1}) 3510(br s) (ν OH), 3080(m), 2980(s), 2940(m), 2875(m), 1725(s) (ν C═O), 1640(s) (ν C═C), 1470(s), 1455(s), 1340(m), 1375(s), 1260(s) (ν C−O−C ester), 1165(s), 1105(s), 995(s); HRMS (ESI) Calcd. for $C_{11}H_{18}O_3Na$ ([M + Na]$^+$) 221.11482, found 221.11485; $C_{11}H_{18}O_3$, M = 198.26 g/mol.

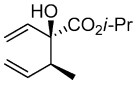

1,5-Hexadiene (±)-**1f**. According to the general procedure for the [2,3]-Wittig rearrangement, the reaction of allyl vinyl ether **11**[46] (2.12 g, 10 mmol) with (i-Pr)$_2$NH (1.69 mL, 12.0 mmol, 1.2 equiv) and n-BuLi (4.78 mL, 11.0 mmol, 1.1 equiv, 2.3 M in hexanes) in THF (20 mL + 30 mL) at −85 → −70 °C (30 min) and −15 °C instead of 0 °C (45 min) provided 1,5-hexadiene (±)-**1f** (1.75 g, 8.3 mmol, 83%) after flash chromatography (cyclohexane/ethyl acetate 200/1): R_f 0.69 (cyclohexane/ethyl acetate 5/1); ^{1}H NMR ($CDCl_3$, 500 MHz, δ) 1.06 (s, 3H), 1.10 (s, 3H), 1.27 (d, J = 6.3 Hz, 3H), 1.30 (d, J = 6.3 Hz, 3H), 3.43 (s, 1H), 5.01 (dd, J = 13.9, 1.1 Hz, 1H), 5.04 (dd, J = 7.5, 1.1 Hz, 1H), eclipsed by 5.07 (spt, J = 6.2, 1H), and 5.23 (dd, J = 10.6, 1.8 Hz, 1H), 5.51 (dd, J = 17.0, 1.8 Hz, 1H), 6.00 (dd, J = 17.4, 10.9 Hz, 1H), 6.12 (dd, J = 17.0, 10.6 Hz, 1H); ^{13}C NMR ($CDCl_3$, 101 MHz, δ) 21.9 (CH_3), 22.0 (CH_3), 22.0 (CH_3), 22.5 (CH_3), 44.3 (C), 70.6 (CH), 80.9 (C), 113.2 (CH_2), 116.4 (CH_2), 135.7 (CH), 143.8 (CH), 174.2 (C); IR (cm^{-1}) 3505(br m) (ν OH), 2985(s), 2935(m), 1715(s) (ν C═O), 1640(w) (ν C═C), 1470(m), 1455(w), 1375(m), 1270(s) (ν C−O−C ester), 1245(s), 1180(s), 1150(s), 1105(s),

dx.doi.org/10.1021/jo3004088 | J. Org. Chem. XXXX, XXX, XXX−XXX

995(m). Anal. Calcd. for $C_{12}H_{20}O_3$: C, 67.9; H, 9.5. Found: C, 67.8; H, 9.5; $C_{12}H_{20}O_3$, M = 212.29 g/mol.

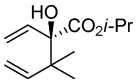

1,5-Hexadiene (±)-**1g**. According to the general procedure for the [2,3]-Wittig rearrangement, the reaction of allyl vinyl ether **12**[42] (1.13 g, 5.7 mmol) with $(i\text{-Pr})_2$NH (0.96 mL, 6.8 mmol, 1.2 equiv) and *n*-BuLi (2.73 mL, 6.3 mmol, 1.1 equiv, 2.3 M in hexanes) in THF (11 mL + 17 mL) at −85 → −70 °C (30 min) and 0 °C (1 h) provided 1,5-hexadiene (±)-**1g** (0.77 g, 3.9 mmol, 69%) after flash chromatography (*n*-pentane/diethyl ether 100/1): R_f 0.57 (cyclohexane/ethyl acetate 5/1); ^{1}H NMR ($CDCl_3$, 400 MHz, δ) 1.26 (d, J = 6.3 Hz, 3H), 1.29 (d, J = 6.3 Hz, 3H), 1.77 (s, 3H), 2.38 (d, J = 13.9 Hz, 1H), 2.61 (d, J = 13.9 Hz, 1H), 3.35 (s, 1H), 4.71−4.91 (m, 2H), 5.06 (spt, J = 6.3 Hz, 1H), 5.17 (dd, J = 10.5, 1.2 Hz, 1H), 5.50 (dd, J = 17.0, 1.2 Hz, 1H), 5.99 (dd, J = 17.0, 10.5 Hz, 1H); ^{13}C NMR ($CDCl_3$, 101 MHz, δ) 21.8 (CH_3), 21.9 (CH_3), 24.2 (CH_3), 46.6 (CH_2), 70.3 (CH), 77.5 (C), 114.8 (CH_2), 115.1 (CH_2), 139.2 (CH), 141.2 (C), 174.4 (C); 3515(br m) (ν OH), 2980(m), 2935(m), 1725(s) (ν C=O), 1645(w) (ν C=C), 1470(w), 1455(m), 1375(m), 1275(m) (ν C−O−C ester), 1210(s), 1145 (s), 1105(s), 1060(m). Anal. Calcd. for $C_{11}H_{18}O_3$: C, 66.6; H, 9.2. Found: C, 66.7; H, 9.4; $C_{11}H_{18}O_3$, M = 198.26 g/mol.

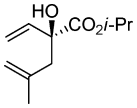

Pd^{II}-Catalyzed Cycloisomerization: Representative Procedure for the Kinetic Experiments. [Pd(allyl)(MeCN)$_2$](BF$_4$),[47] [Pd(MeCN)$_4$](BF$_4$)$_2$,[48] as well as (±)-**1b**,**c** were prepared according to a published procedure.[20]

A solution of hexadiene (±)-*syn*-**1b** (4.5 mg, 0.02 mmol, 1 equiv) in dry $CDCl_3$ (0.2 mL, 10 mL/mmol **1b**) was added to an oven-dried Shigemi tube under argon. The tube was sealed with a septum, and a ^{1}H NMR spectrum was recorded (substrate spectrum). [Pd(MeCN)$_4$](BF$_4$)$_2$ (0.05 mg, 0.001 mmol, 0.05 equiv) was added, and the reaction was monitored by ^{1}H NMR spectroscopy at hourly intervals up to 69 h. The degree of conversion was determined in reference to the substrate spectrum. The NMR resonances could be assigned to (±)-*cis*-**2b**, (±)-*cis*-**3b**, **5b**, and the dimeric cycloisomerization products **6b** and **7b**. For NMR kinetic experiments, ^{1}H NMR measurements were performed with a 500 MHz NMR spectrometer equipped with a 5 mm triple resonance probe H(C,X). All measurements used identical conditions (spectral width 5500 Hz, acquisition time 5.96 s, 64 kB data, 90° pulse width 10.3 μs). The kinetic measurements were performed as array experiments. In this case, the preacquisition time was arrayed from 0 to 88 h. Each spectrum was measured with a single scan. The processing was executed by using zero filling (256 kB).

Dimer (±)-**6b**: R_f 0.51 (cyclohexane/ethyl acetate 5/1); the NMR peak assignment is based on ^{1}H,^{1}H COSY, ^{1}H,^{13}C HSQC, and ^{1}H,^{13}C HMBC experiments; ^{1}H NMR ($CDCl_3$, 500 MHz, δ) 0.84 (t, J = 7.2 Hz, 6H, 9-CH_3+9′CH_3), 1.02−1.22 (m, 4H), 1.23 (d, J = 6.3 Hz, 3H, *i*-Pr-CH_3), eclipsed by 1.22−1.30 (m, 2H) and 1.26 (d, J = 6.3 Hz, 3H, *i*-Pr-CH_3), and 1.29 (d, J = 6.2 Hz, 3H, *i*-Pr-CH_3), and 1.29 (d, J = 6.2 Hz, 3H, *i*-Pr-CH_3), 1.33−1.46 (m, 4H), 1.82−1.93 (m, 2H, 5′/6′-CH_2), 2.00−2.12 (m, 2H, 1′-CH_2), 2.16−2.27 (m, 1H, 4′-CH), 2.27−2.39 (m, 2H, 4-CH+2′-CH), 2.99 (s, 1H, OH), 3.26 (s, 1H, OH), 4.97 (dd, J = 17.2, 1.7 Hz, 1H, 6-CH_2), 5.04 (spt, J = 6.2 Hz, 1H, *i*-Pr-CH), eclipsed by 5.06−5.14 (m, 1H, 6-CH_2), and 5.10 (spt, J = 6.2 Hz, 1H, *i*-Pr-CH), 5.46 (d, J = 15.3 Hz, 1H, 2-CH), 5.50 (ddd, J = 17.3, 9.9, 9.9 Hz, 1H, 5-CH), 5.66 (dt, J = 15.3, 7.3 Hz, 1H, 1-CH); ^{13}C NMR ($CDCl_3$, 126 MHz, δ) 14.0 (9/9′-CH_3), 14.5 (9/9′-CH_3), 20.4 (CH_2), 21.1, (CH_2), 21.9/21.9/21.9/21.9 (4 × *i*-Pr-CH_3), 28.8 (CH_2), 28.8 (CH_2), 31.0 (CH_2), 31.3 (CH_2), 32.2 (1′-CH_2), 48.4 (2′-CH), 48.7 (4′-CH), 51.3 (4-CH), 69.5 (*i*-Pr-CH), 70.2 (*i*-Pr-CH), 79.1 (3-C), 83.4 (3′-C), 117.9 (6-CH_2), 129.2 (1-CH), 131.4 (2-CH), 137.0 (5-CH), 174.9 (C=O), 176.7 (C=O); significant COSY cross peaks 1-C*H*/1′-CH_2, 1-C*H*/5-C*H*, 5-C*H*/4-C*H*, no cross peak observed for 4′-CH_2/2′-CH_2; significant HMBC cross peaks 1′-CH_2/3′-C, 1′-CH_2/2-CH; IR (cm^{-1}) 3515(br m) (ν OH), 2980(m), 2955(s), 2935(m), 2870(m), 1720(s) (ν C=O), 1640(w) (ν C=C), 1465(m), 1375(m), 1255(s) (ν C−O−C ester), 1230(m), 1205(m), 1145(m), 1105(s), 1175(w); HRMS (ESI) Calcd. for $C_{26}H_{45}O_6$ ([M + H]$^+$) 453.32107, found 453.32133; $C_{26}H_{44}O_2$, M = 452.62 g/mol.

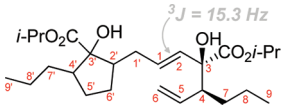

(±)-**7b**: ^{1}H,^{1}H COSY, ^{1}H,^{13}C HSQC, ^{1}H,^{13}C HMBC and NOESY experiments were employed to confirm the NMR peak assignments; ^{1}H NMR ($CDCl_3$, 500 MHz, δ) 0.85 (t, J = 7.2 Hz, 6H, 9/9′-CH_3), 1.13−1.37 (m, 8H, 7/7′-CH_2+8/8′-CH_2), eclipsed by 1.24 (d, J = 6.3 Hz, 6H, 2 × *i*-Pr-CH_3), and 1.28 (d, J = 6.3 Hz, 6H, 2 × *i*-Pr-CH_3), 1.46 (dddd, J = 11.4, 11.4, 11.4, 4.2 Hz, 2H, 5/5′-CH_2^{Re}), 1.67 (dddd, J = 11.50, 11.50, 11.50, 5.10 Hz, 2H, 6/6′-CH_2^{Si}), 1.81−1.90 (m, 2H, 6/6′-CH_2^{Re}), 1.90−2.00 (m, 2H, 5/5′-CH_2^{Re}), 2.31 (tt, J = 8.3 Hz, 2H, 4/4′-CH), 2.75−2.84 (m, 2H, 2/2′-CH), 3.08 (s, 2H, 2 × OH), 5.08 (spt, J = 6.3 Hz, 2H, 2 × *i*-Pr-CH), 5.31 (dd, J = 5.1, 2.4 Hz, 2H, 1/1′-CH); ^{13}C NMR ($CDCl_3$, 126 MHz, δ) 14.5 (9/9′-CH_3), 21.2 (8/8′-CH_2), 21.9 (2 × *i*-Pr-CH_3), 22.1(2 × *i*-Pr-CH_3), 29.0 (6/6′-CH_2), 29.3 (5/5′-CH_2), 31.6 (7/7′-CH_2), 47.8 (4/4′-CH), 53.0 (2/2′-CH), 69.6 (2 × *i*-Pr-CH), 84.8 (3/3′-C), 131.1 (1/1′-CH), 176.0 (2 × C=O); significant COSY cross peaks 1-C*H*/2-C*H*, 2-C*H*/6-CH_2; significant NOESY cross peaks 1-CH/6-CH_2^{Si}, 2-C*H*/4-C*H*, 2-C*H*/6-CH_2^{Re}, 4-C*H*/5-CH_2^{Si}; significant HMBC cross peaks O*H*/4-CH; 6-CH_2^{Si}/1-CH; IR (cm^{-1}) 3470(br s) (ν OH), 29(m), 2930(m), 2870(m), 1715(s) (ν C=O), 1620(m) (ν C=C), 1455(s), 1385(s), 1270(m) (ν C−O−C ester), 1220(m), 1105(s), 1035(s); HRMS (ESI) Calcd. for $C_{26}H_{45}O_6$ ([M + H]$^+$) 453.32107, found 453.32135; $C_{26}H_{44}O_2$, M = 452.62 g/mol.

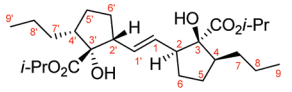

General Procedure for the Pd^{II}-Catalyzed Cycloisomerization. The corresponding Pd-catalyst (0.05 equiv) was added to a solution of 1,5-hexadiene (±)-**1** (1 equiv) in dry CH_2Cl_2 (10 mL/mmol **1**), and the resulting mixture was stirred at the given temperature (reaction at elevated temperatures were carried out in a glass pressure tube, sealed with a Teflon screwcap) until TLC indicated complete conversion of the starting material (3−23 h). The reaction mixture was filtered through a short silica gel-plug (eluent CH_2Cl_2 or ethyl acetate) to remove the catalyst and was then concentrated under reduced pressure. Purification by flash chromatography (cyclohexane/ethyl acetate) afforded the corresponding methylene cyclopentanes (±)-**2**/**2′** along with methyl cyclopentene (±)-**3** and the mono- and double cycloisomerized dimers (±)-**6** and (±)-**7** as a mixture of regioisomers and diastereomers.

Cycloalkenes (±)-**2c** and (±)-**6c**. According to the general procedure for the Pd^{II}-catalyzed cycloisomerization, 1,5-hexadiene (±)-**1c** (110 mg, 0.4 mmol, *syn*/*anti* = 16/84) in CH_2Cl_2 (4 mL) was treated with [Pd(MeCN)$_4$](BF$_4$)$_2$ (8.8 mg, 0.02 mmol, 0.05 equiv) at ambient temperature for 16 h. Purification by flash chromatography (cyclohexane/ethyl acetate 100/1 → 50/1) afforded methylene cyclopentane (±)-**2c**[20] (18 mg, 0.05 mmol, 14%) as a mixture of diastereomers (*cis*/*trans* = 6/94) along with mono cycloisomerized dimer (±)-**6c** (25 mg, 0.09 mmol, 23%) as a mixture of diastereomers (dr = 26/74).

(±)-**6c**: R_f 0.14 (cyclohexane/ethyl acetate 5/1); the NMR peak assignment is based on ^{1}H,^{1}H COSY and ^{1}H,^{13}C HSQC experiments; ^{1}H NMR ($CDCl_3$, 500 MHz, mixture of diastereomers dr = 26/74, δ) 1.16−1.29 (m, 1H, 5′-CH_2), 1.40−1.51 (m, 1H, 6′-CH_2), 1.68−1.81 (m, 1H, 6′-CH_2), 1.89−1.98 (m, 1H, 5′-CH_2), 2.03−2.14 (m, 1H,

dx.doi.org/10.1021/jo3004088 | J. Org. Chem. XXXX, XXX, XXX−XXX

1′-CH_2), 2.16−2.23 (m, 1H, 1′-CH_2), 2.23−2.32 (m, 1H, 2′-CH), 2.40−2.54 (m, 1H, 4′-CH), 2.73 (ddd, J = 9.1, 7.0, 4.2 Hz, 1H, 4-CH), 3.23 (s, 0.7H^{major}, OH), 3.24 (s, 0.3H^{minor}, OH), 3.32−3.43 (m, 2H, 7′-CH_2), 3.53−3.70 (m, 6H, 7-CH_2+OH+OMe), 3.68−3.76 (m, 3H, OMe), 4.35−4.54 (m, 4H, 2 × OCH_2Bn), 5.11−5.19 (m, 2H, 6-CH_2), 5.58 (d, J = 15.3 Hz, 0.7H^{major}, 2-CH), 5.59 (d, J = 15.3 Hz, 0.3H^{minor}, 2-CH), 5.79 (dt, J = 15.3, 7.3 Hz, 1H, 1-CH), 5.83−5.92 (m, 1H, 5-CH), 7.23−7.35 (m, 10H, H^{Ar}); ^{13}C NMR ($CDCl_3$, 126 MHz, mixture of diastereomers dr = 26/74, δ) 27.1/27.1 (5′-CH_2), 29.9/30.1 (6′-CH_2), 31.7/31.8 (1′-CH_2), 47.5/47.7 (2′-CH), 51.5/51.6 (4-CH), 52.7 (OMe), 52.9/53.0 (OMe), 53.6/53.6 (4′-CH), 69.9/70.0 (7-CH_2), 71.3 (7′-CH_2), 73.0/73.1 (OCH_2Bn), 73.4/73.4 (OCH_2Bn), 79.3 (3/3′-C), 82.9/83.0 (3/3′-C), 118.8/118.8 (6-CH_2), 127.6/127.6 (2 × −CH^{Ar}), 127.7/127.8 (4 × −CH^{Ar}), 128.5 (4 × −CH^{Ar}), 130.4/130.5 (2-CH+1-CH), 135.7/135.7 (5-CH), 138.2/138.3 (2 × C^{Ar}), 174.5 (C═O), 176.2 (C═O); significant COSY cross peaks 5-CH/4-CH, 1-CH/1′-CH_2, 7-CH_2/4-CH, 7′-CH_2/4′-CH; IR (cm^{-1}) 3510(br w) (ν OH), 2955(m), 2865(m), 1730(s) (ν C═O), 1495(w), 1455(m), 1435(w), 1385(m), 1365(w), 1255(m) (ν C−O−C ester), 1095(m), 1030(w), 910(s); HRMS (ESI) Calcd. for $C_{32}H_{41}O_8$ ([M + H]$^+$) 553.27959, found 553.28026; $C_{32}H_{40}O_8$, M = 552.66 g/mol.

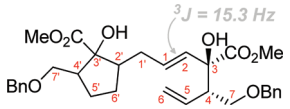

Cycloalkenes (±)-**2d**, (±)-**3d**, (±)-**6d**, and (±)-**7d**. According to the general procedure for the Pd^{II}-catalyzed cycloisomerization, 1,5-hexadiene (±)-**1d** (184 mg, 1 mmol) in dry CH_2Cl_2 (10 mL) was treated with [Pd(MeCN)$_4$](BF$_4$)$_2$ (22.0 mg, 0.05 mmol, 0.05 equiv) at ambient temperature for 23 h. Purification by flash chromatography (cyclohexane/ethyl acetate 100/1 → 5/1) afforded methylene cyclopentane (±)-**2d** (15 mg, 0.08 mmol, 8%) along with a mixed fraction of (±)-**2d** and (±)-**3d** (14 mg, 0.08 mmol, 8%, **2d**/**3d** = 72/28) and a mixed fraction consisting of the dimers (±)-**6d** and (±)-**7d** (58 mg, 0.16 mmol, 32%, **6d**/**7d** = 73/27; dr$_{6d}$ = 74/26) as a mixture of regioisomers and diastereomers.

(±)-**2d**: R_f 0.28 (cyclohexane/ethyl acetate 5/1); the NMR peak assignment is based on ^{1}H,^{1}H COSY and ^{1}H,^{13}C HSQC experiments; ^{1}H NMR ($CDCl_3$, 500 MHz, δ) 1.27 (d, J = 6.2 Hz, 6H, i-Pr-CH_3), 1.89 (t, J = 10.0 Hz, 1H, 2-CH_2), 2.14 (dt, J = 12.6, 9.9 Hz, 1H, 2-CH_2), 2.41−2.54 (m, 2H, 3-CH_2+5-CH_2), 2.56−2.66 (m, 1H, 3-CH_2), 2.83 (d, J = 16.4 Hz, 1H, 5-CH_2), 3.13 (br s, 1H, OH), 4.93 (d, J = 13.7 Hz, 2H, 4′-CH_2), 5.09 (spt, J = 6.2 Hz, 1H, i-Pr-CH); ^{13}C NMR ($CDCl_3$, 126 MHz, δ) 21.8 (2 × i-Pr-CH_3), 31.1 (3-CH_2), 38.7 (2-CH_2), 45.7 (5-CH_2), 69.8 (i-Pr-CH), 81.1 (1-C), 107.1 (4′-CH_2), 149.3 (4-C), 175.9 (C═O); significant COSY cross peaks 4′-CH_2/5-CH_2; IR (cm^{-1}) 3515(br s) (ν OH), 2985(s), 2940(m), 1725(s) (ν C═O), 1645(m) (ν C═C), 1670(m), 1435(m), 1390(m), 1375(s), 1280(s) (ν C−O−C Ester), 1230(s), 1175(s), 1105(s) (ν C−O−C Ether), 995(s); HRMS (ESI) Calcd. for $C_{10}H_{17}O_3$ ([M + H]$^+$) 185.11722, found 185.11720; $C_{10}H_{16}O_3$, M = 184.23 g/mol.

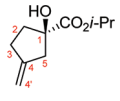

(±)-**2d**/(±)-**3d**: R_f 0.26 (cyclohexane/ethyl acetate 5/1); ^{1}H NMR ($CDCl_3$, 400 MHz, mixture of regioisomers, **2d**/**3d** = 72/28, δ) 1.21−1.33 (m, 6H), 1.79−2.32 (m, 2H), 2.35−2.71 (m, 2H), 2.75−2.98 (m, 1.4H^{2d}+0.3H^{3d}), 3.14 (s, 0.7H^{2d}), 3.35 (s, 0.3H^{3d}), 4.88−4.98 (m, 1.4H^{2d}), 5.01−5.16 (m, 1H), 5.28 (s, 0.3H^{3d}); M = 184.23 g/mol.

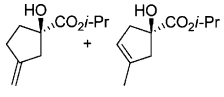

(±)-**6d**/(±)-**7d**: R_f 0.11 (cyclohexane/ethyl acetate 5/1); the NMR peak assignment is based on ^{1}H,^{1}H COSY and ^{1}H,^{13}C HSQC experiments; ^{1}H NMR ($CDCl_3$, 500 MHz, mixture of diastereomers and regioisomers, **6d**/**7d** = 73/27, dr$_{6d}$ = 74/26, δ) (for clarity, only selected resonances of **7d** are listed) 1.21−1.31 (m, 12H, i-Pr-CH_3), 1.39−1.53 (m, 1H, CH_2), 1.62−1.96 (m, 4H, 2 × CH_2), 2.02−2.27 (m, 4H, 1′-CH_2+2′-CH+CH_2), 2.33−2.43 (m, 1H, 4-CH_2), 2.51 (dd, J = 14.0, 7.5 Hz, 1H, 4-CH_2), 2.61−2.71 (m, 0.2H^{minor}, 2/2′-CH), 3.11 (s, 0.8H^{major}, OH), 3.13 (s, 0.2H^{minor}, OH), 3.20 (s, 0.2H^{minor}, OH), 3.28 (s, 0.2H^{minor}, OH), 3.30 (s, 0.8H^{major}, OH), 5.05 (spt, J = 6.2 Hz, 2H, i-Pr-CH), 5.09 (d, J = 12.6 Hz, 2H, 6-CH_2), 5.28−5.34 (m, 0.2H, 1/1′-CH), 5.58 (d, J = 15.3 Hz, 0.8H^{major}, 2-CH), 5.63 (d, J = 15.3 Hz, 0.2H^{minor}, 2-CH), 5.68−5.87 (m, 2H, 5-CH+1-CH); ^{13}C NMR ($CDCl_3$, 126 MHz, mixture of diastereomers and regioisomers, **6d**/**7d** = 73/27, dr$_{6d}$ = 74/26, δ) 21.8/21.9/21.9/21.9 (i-Pr-CH_3), 22.6/23.2 (CH_2), 30.4/30.5/30.6 (CH_2), 31.7/31.8 (1′-CH_2), 37.7 (CH_2), 39.6/39.6 (CH_2), 43.8/44.0 (CH_2), 48.5/48.7 (2′-CH), 53.1 (2/2′-CH), 69.6/69.7 (i-Pr-CH), 70.0/70.2 (i-Pr-CH), 76.4, 82.1/83.7 (3/3′-C), 119.0/119.0 (6-CH_2), 129.6/129.7 (1-CH), 131.2/131.4 (2-CH), 131.6 (1/1′-CH), 132.4/132.5 (5-CH), 174.4/174.5 (C═O), 176.1 (C═O), 176.8/176.9 (C═O); significant COSY cross peaks 1-CH/1′-CH_2; 5-CH/4-CH_2, 1-CH/2-CH; IR (cm^{-1}) 3505(br s) (ν OH), 2980(s), 2940(s), 2875(m), 1725(s) (ν C═O), 1640(w) (ν C═C), 1470(m), 1455(m), 1375(s), 1230(s) (ν C−O−C ester), 1180(s), 1145(s), 1110(s), 1035(m); HRMS (ESI) Calcd. for $C_{20}H_{33}O_6$ ([M + H]$^+$) 369.22717, found 369.22835; $C_{20}H_{32}O_6$, M = 368.46 g/mol.

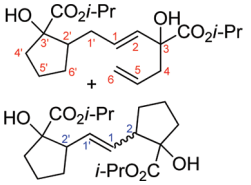

Cycloalkenes (±)-**2e**, (±)-**2′e**, (±)-**3e**, and (±)-**7e**. According to the general procedure for the Pd^{II}-catalyzed cycloisomerization, 1,5-hexadiene (±)-**1e** (100 mg, 0.5 mmol, *syn*/*anti* = 77/23) in dry CH_2Cl_2 (5 mL) was treated with [Pd(MeCN)$_4$](BF$_4$)$_2$ (11.2 mg, 0.05 mmol, 0.05 equiv) at ambient temperature for 3 h. Purification by flash chromatography (*n*-pentane/diethyl ether 50/1 → 5/1) afforded cycloalkenes (±)-**2e**, (±)-**2′e**, and (±)-**3e** (11 mg, 0.06 mmol, 11%) as a mixture of regioisomers and diastereomers (**2e**/**2′e**/**3e** = 61/14/24) along with (±)-**7e** (37 mg, 0.1 mmol, 37%). Subsequent recrystallization of (±)-**7e** by vapor diffusion technique from isohexane and ethyl acetate provided colorless crystals suitable for an X-ray crystal structure analysis.

(±)-**2e**, (±)-**2′e**, and (±)-**3e**: R_f 0.37 (cyclohexane/ethyl acetate 5/1); the NMR peak assignment is based on ^{1}H,^{1}H COSY and ^{1}H,^{13}C HSQC experiments; ^{1}H NMR ($CDCl_3$, 500 MHz, mixture of regio- and diastereomers, **2e**/**2′e**/**3e** = 61/14/24, δ) 0.88 (t, J = 7.1 Hz, 3H^{2e+3e}), 0.94−1.05 (m, 3H^{2e}), 1.18−1.32 (m, 6H), 1.68 (br s, 3H^{3e}), 1.87 (ddd, J = 13.0, 7.5, 3.6 Hz, 1H^{2e}), 2.17 (dt, J = 13.1, 10.3 Hz, 1H^{2e}), 2.32−2.64 (m, 2H), 2.71−2.89 (m, 1H), 2.93 (dd, J = 16.6, 2.1 Hz, 1H^{3e}), 3.01 (s, 1H^{2e}), 3.13 (s, 1H^{3e}), 3.20 (s, 1H^{2e}), 3.48 (q, J = 6.9 Hz, 1H), 4.77 (d, J = 2.3 Hz, 0.2H^{minder,2e}), 4.82 (d, J = 2.7 Hz, 0.8H^{haupt,2e}), 4.84 (d, J = 2.3 Hz, 0.2H^{minder,2e}), 4.96 (d, J = 2.3 Hz, 0.8H^{haupt,2e}), 5.00 (t, J = 2.3 Hz, 1H^{2e}), 5.03 (t, J = 2.3 Hz, 1H^{2e}), 5.07−5.15 (m, 1H), 5.33 (s, 1H^{3e}); IR (cm^{-1}) 3510(br s) (ν OH), 2980(s), 2940(s), 2875(m), 1725(s) (ν C═O), 1640(s) (ν C═C), 1470(m), 1455(m), 1455(s), 1400(m), 1375(s), 1260(s) (ν C−O−C ester), 1165(s), 1145(s), 1105(s) (ν C−O−C Ether), 995(s); HRMS (ESI) Calcd. for $C_{11}H_{19}O_3$ ([M + H]$^+$) 199.13287, found 199.13277; $C_{11}H_{18}O_3$, M = 198.26 g/mol.

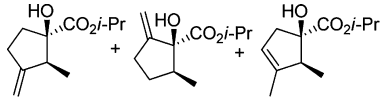

(±)-*cis*-**7e**: R_f 0.20 (cyclohexane/ethyl acetate 5/1); the NMR peak assignment is based on ^{1}H,^{1}H COSY and ^{1}H,^{13}C HSQC experiments;

dx.doi.org/10.1021/jo3004088 | J. Org. Chem. XXXX, XXX, XXX−XXX

^{1}H NMR ($CDCl_3$, 500 MHz, δ) 0.88 (d, J = 6.9 Hz, 6H, 7/7′-CH_3), 1.24 (d, J = 6.2 Hz, 6H, i-Pr-CH_3), 1.25 (d, J = 6.2 Hz, 6H, i-Pr-CH_3), 1.45 (ddt, J = 11.6, 11.5, 4.2 Hz, 2H, 5/5′-CH_2), 1.65 (ddt, J = 12.2, 11.1, 5.0 Hz, 2H, 6/6′-CH_2), 1.79−1.87 (m, 2H, 6/6′-CH_2), 1.87−1.94 (m, 2H, 5/5′-CH_2), 2.36 (tq, J = 9.6, 6.9 Hz, 2H, 4/4′-CH), 2.85 (dddd, J = 10.5, 8.0, 5.6, 2.3 Hz, 2H, 2/2′-CH), 2.92 (s, 2H, OH), 5.07 (spt, J = 6.2 Hz, 2H, i-Pr-H), 5.41 (dd, J = 5.2, 2.5 Hz, 2H, 1/1′-CH); ^{13}C NMR ($CDCl_3$, 126 MHz, δ) 12.9 (7/7′-CH_3), 22.0 (2 × i-Pr-CH_3), 22.1 (2 × i-Pr-CH_3), 29.2 (6/6′-CH_2), 30.6 (5/5′-CH_2), 43.0 (4/4′-CH), 52.7 (2/2′-CH), 69.5 (2 × i-Pr-CH), 85.1 (3/3′-C), 130.8 (1/1′-CH), 175.5 (2 × C═O); significant COSY cross peaks 1-CH/2-CH, 2-CH/6-CH_2, 4-CH/7-CH_3, $C_{22}H_{36}O_6$, M = 396.52 g/mol.

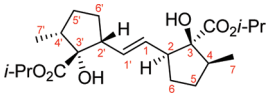

Cycloalkenes (±)-**2f**, (±)-**2′f**, (±)-**3f**, (±)-**6f**, and (±)-**7f**. According to the general procedure procedure for the Pd^{II}-catalyzed cycloisomerization, 1,5-hexadiene (±)-**1f** (100 mg, 0.47 mmol) in dry CH_2Cl_2 (4.7 mL) was treated with $[Pd(MeCN)_4](BF_4)_2$ (10.4 mg, 0.024 mmol, 0.05 equiv) and PCy_3 (6.7 mg, 0.024 mmol, 0.05 equiv), at room temperature for 6 h. Purification by flash chromatography (cyclohexane/ethyl acetate 100/1 → 5/1) afforded regioisomeric methylene cyclopentane (±)-**2f′** (6 mg, 0.03 mmol, 6%) along with a mixed fraction of cycloalkenes (±)-**2f** and (±)-**3f** (21 mg, 0.1 mmol, 21%, **2f**/**3f** = 89/11) and a dimer fraction containing (±)-**6f** and (±)-**7f** (52 mg, 0.13 mmol, 52%) as mixture of regioisomers and diastereomers (**6f**/**7f** = 60/40, dr_{7f} = 66/34). Subsequent recrystallization by vapor diffusion technique from isohexane and ethyl acetate provided colorless crystals of (±)-*cis*-**7f** suitable for an X-ray crystal structure analysis.

(±)-**2′f**: R_f 0.77 (cyclohexane/ethyl acetate 5/1); the NMR peak assignment is based on ^{1}H,^{1}H COSY, ^{1}H,^{13}C HSQC, and ^{1}H,^{13}C HMBC experiments; ^{1}H NMR ($CDCl_3$, 500 MHz, δ) 0.93 (s, 6H, 2 × 7-CH_3), 1.23 (d, J = 6.3 Hz, 3H, i-Pr-CH_3), 1.30 (d, J = 6.3 Hz, 3H, i-Pr-CH_3), 1.54 (ddd, J = 12.4, 6.9, 5.2 Hz, 1H, 5-CH_2), 1.94 (dt, J = 12.4, 9.7 Hz, 1H, 5-CH_2), 2.47−2.53 (m, 2H, 6-CH_2), 3.72 (s, 1H, OH), 5.03 (t, J = 2.0 Hz, 1H, 1-CH_2), 5.07 (spt, J = 6.3 Hz, 1H, i-Pr-CH), 5.15 (t, J = 2.51 Hz, 1H, 1-CH_2); ^{13}C NMR ($CDCl_3$, 126 MHz, δ) 21.7 (i-Pr-CH_3), 21.9 (i-Pr-CH_3), 22.6 (7-CH_3), 24.1 (7-CH_3), 27.3 (6-CH_2), 35.6 (6-CH_2), 44.8 (4-C), 70.2 (i-Pr-CH), 85.9 (3-C), 109.2 (1-CH_2), 152.5 (2-C), 175.0 (C═O); significant COSY cross peaks 1-CH_2/6-CH_2; significant HMBC cross peaks 1-CH_2/6-C, 1-CH_2/3-C; IR (cm^{-1}) 3480(br m) (ν OH), 2960(s), 2930(s), 2870(s), 1725(s) (ν C═O), 1635(w) (ν C═C), 1465(s), 1385(s), 1375(s), 1270(s) (ν C−O−C ester), 1235(s), 1180(s), 1145(s), 1110(s), 1050(s); HRMS (ESI) Calcd. for $C_{12}H_{20}O_3Na$ ([M + Na]$^+$) 235.13047, found 235.13027; $C_{12}H_{20}O_3$, M = 212.29 g/mol.

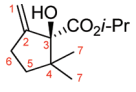

(±)-**2f**: R_f 0.49 (cyclohexane/ethyl acetate 5/1); the NMR peak assignment is based on ^{1}H,^{1}H COSY, ^{1}H,^{13}C HSQC, and ^{1}H,^{13}C HMBC experiments; ^{1}H NMR ($CDCl_3$, 500 MHz, δ) 0.95 (s, 3H, 7-CH_3), 1.09 (s, 3H, 7-CH_3), 1.25 (d, J = 6.3 Hz, 3H, i-Pr-CH_3), 1.27 (d, J = 6.3 Hz, 3H, i-Pr-CH_3), 1.92 (ddd, J = 13.6, 10.0, 6.0 Hz, 1H, 2-CH_2), 2.23 (ddd, J = 13.6, 9.6, 6.7 Hz, 1H, 2-CH_2), 2.47−2.64 (m, 2H, 1-CH_2), 3.19 (s, 1H, OH), 4.78 (t, J = 2.4 Hz, 1H, 6-CH_2), 4.81 (t, J = 2.0 Hz, 1H, 6-CH_2), 5.06 (spt, J = 6.3 Hz, 1H, i-Pr-CH); ^{13}C NMR ($CDCl_3$, 126 MHz, δ) 21.9 (i-Pr-CH_3), 22.0 (i-Pr-CH_3), 23.1 (7-CH_3), 24.1 (7-CH_3), 28.5 (1-CH_2), 32.3 (2-CH_2), 49.5 (4-C), 69.8 (i-Pr-CH), 85.4 (3-C), 104.4 (6-CH_2), 158.9 (5-C), 175.1 (C═O); significant COSY cross peaks 6-CH_2/1-CH_2; significant HMBC cross peaks 6-CH_2/4-C, 6-CH_2/1-CH_2, OH/2-CH_2; IR (cm^{-1}) 3510(br s) (ν OH), 2980(s), 2935(s), 2875(s), 1715(s) (ν C═O), 1655(m) (ν C═C), 1465(s), 1375(s), 1255(s) (ν C−O−C ester), 1195(s), 1145(s), 1110(s). Anal. Calcd. for $C_{12}H_{20}O_3$: C, 67.9; H, 9.5. Found: C, 67.9; H, 9.6; $C_{12}H_{20}O_3$, M = 212.29 g/mol.

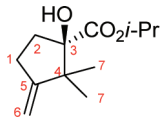

(±)-**3f**: R_f 0.49 (cyclohexane/ethyl acetate 5/1); the NMR peak assignment is based on ^{1}H,^{1}H COSY, ^{1}H,^{13}C HSQC, and ^{1}H,^{13}C HMBC experiments; ^{1}H NMR ($CDCl_3$, 500 MHz, δ) 0.90 (s, 3H, 7-CH_3), 1.08 (s, 3H, 7-CH_3), 1.28 (d, J = 6.3 Hz, 3H, i-Pr-CH_3), eclipsed by 1.28 (d, J = 6.3 Hz, 3H, i-Pr-CH_3), 1.61 (d, J = 1.7 Hz, 3H, 6-CH_3), 2.35 (dt, J = 16.6, 2.0 Hz, 1H, 2-CH_2), 3.02 (dt, J = 16.6, 2.1 Hz, 1H, 2-CH_2), eclipsed by 3.03 (s, 1H, OH), 5.09 (spt, J = 6.3 Hz, 1H, i-Pr-CH), 5.29 (br s, 1H, 1-CH); ^{13}C NMR ($CDCl_3$, 126 MHz, δ) 12.8 (6-CH_3), 19.4 (7-CH_3), 21.9 (i-Pr-CH_3), 22.0 (i-Pr-CH_3), 22.6 (7-CH_3), 40.5 (2-CH_2), 52.8 (4-C), 69.4 (i-Pr-CH), 86.1 (3-C), 119.9 (1-CH), 144.5 (5-C), 174.5 (C═O); significant COSY cross peaks 1-CH/6-CH_3; significant HMBC cross peaks 1-CH/4-C, 1-CH/3-C, OH/2-CH_2; IR (cm^{-1}) 3500(br s) (ν OH), 2980(s), 2935(s), 2875(s), 1765(m) (ν C═C), 1725(s) (ν C═O), 1465(s), 1385(s), 1375(s), 1265(s) (ν C−O−C ester), 1205(s), 1185(s), 1145(s), 1110(s), 1055(s), 1020(s); Calcd. for $C_{12}H_{21}O_3$ ([M + H]$^+$) 213.14852, found 213.14818; $C_{12}H_{20}O_3$, M = 212.29 g/mol.

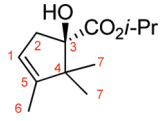

(±)-**6f**: R_f 0.40 (cyclohexane/ethyl acetate 5/1); the NMR peak assignment is based on ^{1}H,^{1}H COSY and ^{1}H,^{13}C HSQC experiments; ^{1}H NMR ($CDCl_3$, 500 MHz, δ) 0.96 (s, 3H, 7/7′-CH_3), 0.98 (s, 3H, 7/7′-CH_3), 1.03 (s, 3H, 7/7′-CH_3), 1.07 (s, 3H, 7/7′-CH_3), 1.26 (d, J = 6.3 Hz, 3H, i-Pr-CH_3), eclipsed by 1.26−1.28 (m, 6H, 2 × i-Pr-CH_3), and 1.29 (d, J = 6.3 Hz, 3H, i-Pr-CH_3), 1.37−1.42 (m, 1H, 6′-CH_2), 1.46 (dt, J = 8.7, 4.4 Hz, 1H, 5′-CH_2), 1.73−1.82 (m, 1H, 5′-CH_2), 1.85−1.95 (m, 1H, 6′-CH_2), 2.08−2.22 (m, 2H, 1′-CH_2), 2.76 (dddd, J = 9.0, 9.0, 9.0, 6.0 Hz, 1H, 2′-CH), 3.03 (s, 1H, OH), 3.41 (s, 1H, OH), 4.98 (dd, J = 16.4, 1.3 Hz, 1H, 6-CH_2), eclipsed by 5.01−5.03 (m, 1H, 6-CH_2), and 5.05 (spt, J = 6.3 Hz, 1H, i-Pr-CH), and 5.07 (spt, J = 6.2 Hz, 1H, i-Pr-CH_3), 5.73 (d, J = 15.3 Hz, 1H, 2-CH), 5.82 (dt, J = 15.3, 7.3 Hz, 1H, 1-CH), 5.97 (dd, J = 17.5, 10.9 Hz, 1H, 5-CH); ^{13}C NMR ($CDCl_3$, 126 MHz, δ) 21.9/22.0/22.0/22.1 (4 × i-Pr-CH_3), 22.1/22.4/22.6/26.7 (4 × 7/7′-CH_3), 27.6 (6′-CH_2), 33.5 (1′-CH_2), 38.8 (5′-CH_2), 44.1 (2′-CH), 44.5/47.8 (4-C+4′-C), 69.6 (i-Pr-CH), 70.5 (i-Pr-CH), 80.4/86.2 (3-C+3′-C), 113.0 (6-CH_2), 128.3 (2-CH), 131.1 (1-CH), 144.1 (5-CH), 174.6 (C═O), 174.8 (C═O); significant COSY cross peaks 5-CH/6-CH, 1-CH/1′-CH_2, 2′-CH/1′-CH_2, 2′-CH/6′-CH_2; IR (cm^{-1}) 3510(br s) (ν OH), 2980(s), 2940(s), 2875(s), 1715(s) (ν C═O), 1640(w) (ν C═C), 1470(s), 1385(s), 1375(s), 1270(s) (ν C−O−C ester), 1225(s), 1180(m), 1145(s), 1110(s); Calcd. for $C_{24}H_{41}O_6$ ([M + H]$^+$) 425.28977, found 425.28963; $C_{24}H_{40}O_6$, M = 424.57 g/mol.

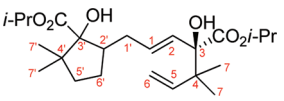

(±)-**7f**: R_f 0.40 (cyclohexane/ethyl acetate 5/1); the NMR peak assignment is based on ^{1}H,^{1}H COSY, ^{1}H,^{13}C HSQC, and ^{1}H,^{13}C HMBC experiments; ^{1}H NMR ($CDCl_3$, 500 MHz, δ) 0.99 (s, 12H, 2 × 7-CH_3+2 × 7′-CH_3), 1.26 (d, J = 6.3 Hz, 12H, 4 × i-Pr-CH_3), 1.49 (td, J = 8.2, 4.0 Hz, 2H, 5/5′-CH_2), 1.59−1.68 (m, 2H, 6/6′-CH_2), 1.76−1.84 (m, 2H, 5/5′-CH_2), 1.85−1.94 (m, 2H, 6/6′-CH_2), 2.99 (s, 2H, OH), 3.19−3.28 (m, 2H, 2/2′-CH), 5.03 (spt, J = 6.3 Hz, 2H, i-Pr-CH), 5.49 (dd, J = 4.9, 2.3 Hz, 2H, 1/1′-CH); ^{13}C NMR ($CDCl_3$, 126 MHz, δ) 22.1 (4 × i-Pr-CH_3), 22.6 (7/7′-CH_3), 27.2 (7/7′-CH_3), 27.8 (6/6′-CH_2), 39.0 (5/5′-CH_2), 47.6 (2/2′-CH), 48.5 (4/4′-C), 69.7 (2 × i-Pr-CH), 87.4 (3/3′-C), 131.2 (1/1′-CH), 174.4 (2 × C═O);

dx.doi.org/10.1021/jo3004088 | J. Org. Chem. XXXX, XXX, XXX−XXX

significant COSY cross peaks 1-C*H*/2-C*H*, 2-C*H*/6-CH_2; significant HMBC cross peaks 1′-C*H*/2-CH, O*H*/2-CH; IR (cm^{-1}) 3525(br s) (ν OH), 2980(s), 2960(s), 2870(s), 1710(s) (ν C═O), 1620(w) (ν C═C), 1470(s), 1385(m, 1375(m), 1280(s) (ν C−O−C ester), 1230(s), 1180(w), 1145(w), 1105(s); Calcd. for $C_{24}H_{41}O_6$ ([M + H]$^+$) 425.28977, found 425.28993; $C_{24}H_{40}O_6$, M = 424.57 g/mol.

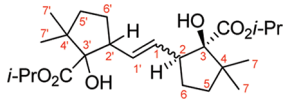

(±)-*cis*-**7f**: R_f 0.29 (cyclohexane/ethyl acetate 5/1); the NMR peak assignment is based on ^{1}H,^{1}H COSY and ^{1}H,^{13}C HSQC experiments; ^{1}H NMR ($CDCl_3$, 500 MHz, δ) 0.99 (s, 6H, 2 × 7/7′-CH_3), 1.00 (s, 6H, 2 × 7/7′-CH_3), 1.25 (d, J = 6.3 Hz, 6H, 2 × *i*-Pr-CH_3), 1.27 (d, J = 6.3 Hz, 6H, 2 × *i*-Pr-CH_3), 1.46−1.53 (m, 2H, 5/5′-CH_2), 1.55−1.65 (m, 2H, 6/6′-CH_2), 1.76−1.90 (m, 4H, 5/5′-CH_2+6/6′-CH_2), 3.00 (s, 2H, OH), 3.19−3.30 (m, 2H, 2/2′-CH), 5.07 (spt, J = 6.3 Hz, 2H, *i*-Pr-CH), 5.50 (dd, J = 5.2, 2.5 Hz, 2H, 1/1′-CH); ^{13}C NMR ($CDCl_3$, 126 MHz, δ) 22.1 (2 × *i*-Pr-CH_3), 22.2 (2 × *i*-Pr-CH_3), 22.7 (2 × 7/7′-CH_3), 27.2 (2 × 7/7′-CH_3), 27.9 (6/6′-CH_2), 39.0 (5/5′-CH_2), 47.5 (2/2′-CH), 48.6 (4/4′-CH), 69.5 (*i*-Pr-CH), 87.4 (3/3′-C), 131.3 (1/1′-CH), 174.4 (2 × C═O); significant COSY cross peaks 1-C*H*/2-C*H*, 2-C*H*/6-CH_2; IR (cm^{-1}) 3505(br s) (ν OH), 2980(s), 2975(s), 1715(s) (ν C═O), 1640(m) (ν C═C), 1470(s), 1415(m), 1385(s), 1270(s) (ν C−O−C ester), 1180(s), 1145(s), 1105(s), 1045(s), 980(s), 910(s); Calcd. for $C_{24}H_{41}O_6$ ([M + H]$^+$) 425.28977, found 425.28956; $C_{24}H_{40}O_6$, M = 424.57 g/mol.

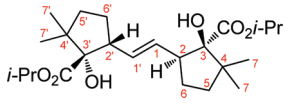

Dimer (±)-**8**. According to the general procedure for the Pd^{II}-catalyzed cycloisomerization, 1,5-hexadiene (±)-**1g** (100 mg, 0.5 mmol) in dry CH_2Cl_2 (5 mL) was treated with $[Pd(MeCN)_4](BF_4)_2$ (11.2 mg, 0.025 mmol, 0.05 equiv) at ambient temperature for 3 days. Purification by flash chromatography (cyclohexane/ethyl acetate 100/1 → 50/1) afforded (±)-**8** (50 mg, 0.13 mmol, 50%) as a mixture of diastereomers (dr = 71/29): R_f 0.2 (cyclohexane/ethyl acetate 5/1); the NMR peak assignment is based on ^{1}H,^{1}H COSY and ^{1}H,^{13}C HSQC experiments; ^{1}H NMR ($CDCl_3$, 500 MHz, mixture of diastereomers, dr = 71/29, δ) 1.01 (s, 0.9H^{minor}, 7′-CH_3), 1.10 (s, 2.1H^{major}, 7′-CH_3), 1.20−1.31 (m, 12H, 4 × *i*-Pr-CH_3), 1.35−1.70 (m, 2H, 4′-CH_2), 1.50−2.24 (m, 6H, 6′-CH_2+1′-CH_2+2′-CH_2), 1.76 (s, 3H, 7-CH_3), 2.39 (d, J = 13.9 Hz, 1H, 4-CH_2), 2.59 (d, J = 13.9 Hz, 1H, 4-CH_2), 3.18 (br s, 1H, OH), 3.35 (br s, 1H, OH), 4.77 (s, 1H, 6-CH_2), 4.85 (s, 1H, 6-CH_2), 5.05 (spt, J = 6.3 Hz, 1H, *i*-Pr-CH), eclipsed by 5.06 (spt, J = 6.3 Hz, 1H, *i*-Pr-CH), 5.62 (d, J = 15.3 Hz, 0.7H^{major}, 2-CH), 5.63 (d, J = 14.9 Hz, 0.3H^{minor}, 2-CH), 5.85−5.96 (m, 1H, 1-CH); ^{13}C NMR ($CDCl_3$, 126 MHz, mixture of diastereomers, dr = 71/29, δ) 21.8/21.8 (2 × *i*-Pr-CH_3), 21.9/21.9 (2 × *i*-Pr-CH_3), 24.2 (7-CH_3), 27.1/27.2 (7′-CH_3), 38.6/38.7 (4′-CH_2), 38.8/39.0 (1′/2′-CH_2), 42.9/43.0 (5′-C), 45.0 (6′-CH_2), 46.9/46.9 (4-CH_2), 51.8/51.8 (1′/2′-CH_2), 69.6/69.6 (*i*-Pr-CH), 70.1/70.1 (*i*-Pr-CH), 82.2/82.3 (3-C+3′-C), 114.9/115.0 (6-CH_2), 128.0/128.2 (1-CH), 133.7/133.8 (2-CH), 141.3/141.4 (5-C), 174.7/174.7 (C═O), 176.9/176.9 (C═O); significant COSY cross peaks 1-C*H*/6′-CH_2, 6-CH_2/7-CH_3; IR (cm^{-1}) 3510(br s) (ν OH), 2980(s), 2870(s), 1725(s) (ν C═O), 1645(w) (ν C═C), 1455(s), 1375(s), 1275(s) (ν C−O−C ester), 1215(s), 1145(s), 1105(s), 1070(s); Calcd. for $C_{22}H_{37}O_6$ ([M + H]$^+$) 397.25847, found 397.25820; $C_{22}H_{36}O_6$, M = 396.52 g/mol.

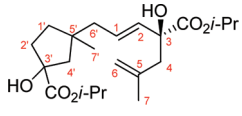

■ ASSOCIATED CONTENT

Supporting Information

Computational details, copies of NMR as well as IR spectra, and CIF files for compounds **7e**,**f**. This material is available free of charge via the Internet at http://pubs.acs.org.

■ AUTHOR INFORMATION

Corresponding Author

*E-mail: bjoern.nelson@tu-dortmund.de; martin.hiersemann@tu-dortmund.de.

Notes

The authors declare no competing financial interest.

■ ACKNOWLEDGMENTS

We are grateful to the Deutsche Forschungsgemeinschaft (HI628/10-1) and the Technische Universität Dortmund for financial support of this research. Computations were performed on the LiDOng cluster at the ITMC of the TU Dortmund.

■ REFERENCES

(1) (a) Trost, B. M. *Chem. Soc. Rev* **1982**, *11*, 141−170. (b) Hudlicky, T.; Price, J. D. *Chem. Rev.* **1989**, *89*, 1467−1486. (c) Lautens, M.; Klute, W.; Tam, W. *Chem. Rev.* **1996**, *96*, 49−92. (d) Heasley, B. *Eur. J. Org. Chem.* **2009**, 1477−1489.

(2) For selected reviews on 1,*n*-enyne, -diyne, and -diene cycloisomerization, see: (a) Trost, B. M. *Acc. Chem. Res.* **1990**, *23*, 34−42. (b) Trost, B. M.; Krische, M. J. *Synlett* **1998**, 1−16. (c) Widenhoefer, R. A. *Acc. Chem. Res.* **2002**, *35*, 905−913. (d) Aubert, C.; Buisine, O.; Malacria, M. *Chem. Rev.* **2002**, *102*, 813−834. (e) Lloyd-Jones, G. C. *Org. Biomol. Chem.* **2003**, *1*, 215−236. (f) Schmidt, B. *Angew. Chem., Int. Ed. Engl.* **2003**, *42*, 4996−4999. (g) Ma, S.; Yu, S.; Gu, Z. *Angew. Chem., Int. Ed. Engl.* **2006**, *45*, 200−203. (h) Zhang, L.; Sun, J.; Kozmin, S. A. *Adv. Synth. Catal.* **2006**, *348*, 2271−2296. (i) Michelet, V.; Toullec, P. Y.; Genet, J.-P. *Angew. Chem., Int. Ed. Engl.* **2008**, *47*, 4268−4315.

(3) (a) Trost, B. M. *Science* **1991**, *254*, 1471−1477. (b) Trost, B. M. *Angew. Chem., Int. Ed. Engl.* **1995**, *34*, 259−281. (c) Trost, B. M. *Acc. Chem. Res.* **2002**, *35*, 695−705.

(4) Nickel: (a) Müller, H.; Wittenberg, D.; Seibt, H.; Scharf, E. *Angew. Chem.* **1965**, *77*, 318−323. (b) Radetich, B.; RajanBabu, T. V. *J. Am. Chem. Soc.* **1998**, *120*, 8007−8008. (c) Neas, D.; Turský, M.; Tilerová, I.; Kotora, M. *New J. Chem.* **2006**, *30*, 671−674. (d) Böing, C.; Hahne, J.; Francis, G.; Leitner, W. *Adv. Synth. Catal.* **2008**, *350*, 1073−1080.

(5) Ruthenium: (a) Yamamoto, Y.; Ohkoshi, N.; Kameda, M.; Itoh, K. *J. Org. Chem.* **1999**, *64*, 2178−2179. (b) Cetinkaya, B.; Demir, S.; Özdemir, I.; Toupet, L.; Semeril, D.; Bruneau, C.; Dixneuf, P. H. *New J. Chem.* **2001**, *25*, 519−521. (c) Yamamoto, Y.; Nakagai, Y.-i.; Ohkoshi, N.; Itoh, K. *J. Am. Chem. Soc.* **2001**, *123*, 6372−6380. (d) Cietinkaya, B.; Demir, S.; Özdemir, I.; Toupet, L.; Semeril, D.; Bruneau, C.; Dixneuf, P. H. *Chem.—Eur. J.* **2003**, *9*, 2323−2330. (e) Michaut, M.; Santelli, M.; Parrain, J.-L. *Tetrahedron Lett.* **2003**, *44*, 2157−2159. (f) Yamamoto, Y.; Nakagai, Y.-i.; Itoh, K. *Chem.—Eur. J.* **2004**, *10*, 231−236. (g) Terada, Y.; Arisawa, M.; Nishida, A. *J. Org. Chem.* **2006**, *71*, 1269−1272. (h) Arisawa, M.; Terada, Y.; Takahashi, K.; Nakagawa, M.; Nishida, A. *J. Org. Chem.* **2006**, *71*, 4255−4261. (i) Fairlamb, I. J. S.; McGlacken, G. P.; Weissberger, F. *Chem. Commun.* **2006**, 988−990. (j) Miao, X.; Feder-Kubis, J.; Fischmeister, C.; Pernak, J.; Dixneuf, P. H. *Tetrahedron* **2008**, *64*, 3687−3690.

(6) Platinum: (a) Kerber, W. D.; Koh, J. H.; Gagne, M. R. *Org. Lett.* **2004**, *6*, 3013−3015. (b) Kerber, W. D.; Gagne, M. R. *Org. Lett.* **2005**, *7*, 3379−3381. (c) Feducia, J. A.; Campbell, A. N.; Doherty, M. Q.; Gagne, M. R. *J. Am. Chem. Soc.* **2006**, *128*, 13290−13297. (d) Bell, F.; Holland, J.; Green, J. C.; Gagne, M. R. *Organometallics* **2009**, *28*, 2038−2045.

(7) Rhodium: (a) Bright, A.; Malone, J. F.; Nicholson, J. K.; Powell, J.; Shaw, B. L. *J. Chem. Soc., Chem. Commun.* **1971**, 712−713. (b) Grigg, R.; Mitchell, T. R. B.; Ramasubbu, A. *J. Chem. Soc., Chem. Commun.* **1980**, 27−28. (c) Sato, Y.; Oonishi, Y.; Mori, M. *Organometallics* **2003**, *22*, 30−32. (d) Oonishi, Y.; Taniuchi, A.; Mori, M.; Sato, Y. *Tetrahedron Lett.* **2006**, *47*, 5617−5621. (e) Oonishi, Y.; Saito, A.; Mori, M.; Sato, Y. *Synthesis* **2009**, 969−979.
(8) Titanium: (a) Okamoto, S.; Livinghouse, T. *J. Am. Chem. Soc.* **2000**, *122*, 1223−1224. (b) Okamoto, S.; Livinghouse, T. *Organometallics* **2000**, *19*, 1449−1451.
(9) Palladium: (a) Schmitz, E.; Heuck, U.; Habisch, D. *J. Prakt. Chem.* **1976**, *318*, 471−478. (b) Schmitz, E.; Urban, R.; Heuck, U.; Zimmermann, G.; Gründemann, E. *J. Prakt. Chem.* **1976**, *318*, 185−192. (c) Grigg, R.; Mitchell, T. R. B.; Ramasubbu, A. *J. Chem. Soc., Chem. Commun.* **1979**, 669−670. (d) Grigg, R.; Malone, J. F.; Mitchell, T. R. B.; Ramasubbu, A.; Scott, R. M. *J. Chem. Soc., Perkin Trans. 1* **1984**, 1745−1754. (e) Takacs, J. M.; Zhu, J.; Chandramouli, S. *J. Am. Chem. Soc.* **1992**, *114*, 773−774. (f) Heumann, A.; Moukhliss, M. *Synlett* **1998**, 1211−1212. (g) Widenhoefer, R. A.; Perch, N. S. *Org. Lett.* **1999**, *1*, 1103−1105. (h) Kisanga, P.; Widenhoefer, R. A. *J. Am. Chem. Soc.* **2000**, *122*, 10017−10026. (i) Bray, K. L.; Charmant, J. P. H.; Fairlamb, I. J. S.; Lloyd-Jones, G. C. *Chem.—Eur. J.* **2001**, *7*, 4205−4215. (j) Bray, K. L.; Fairlamb, I. J. S.; Lloyd-Jones, G. C. *Chem. Commun.* **2001**, 187−188. (k) Bray, K. L.; Lloyd-Jones, G. C. *Eur. J. Org. Chem.* **2001**, 1635−1642. (l) Bray, K. L.; Fairlamb, I. J. S.; Kaiser, J.-P.; Lloyd-Jones, G. C.; Slatford, P. A. *Top Catal.* **2002**, *19*, 49−59. (m) Fairlamb, I. J. S.; Grant, S.; Tommasi, S.; Lynam, J. M.; Bandini, M.; Dong, H.; Lin, Z.; Whitwood, A. C. *Adv. Synth. Catal.* **2006**, *348*, 2515−2530. (n) Song, Y.-J.; Jung, I. G.; Lee, H.; Lee, Y. T.; Chung, Y. K.; Jang, H.-Y. *Tetrahedron Lett.* **2007**, *48*, 6142−6146. (o) Feng, L.; Gan, Z.; Nie, X.; Sun, P.; Bao, J. *Catal. Commun.* **2010**, *11*, 555−559.
(10) Ziegler, K. *Angew. Chem.* **1956**, *68*, 721−729.
(11) (a) Mach, K.; Sedmera, P.; Petrusova, L.; Antropiusova, H.; Hanus, V.; Turecek, F. *Tetrahedron Lett.* **1982**, *23*, 1105−1108. (b) Lehmkuhl, H.; Tsien, Y.-L. *Chem. Ber.* **1983**, *116*, 2437−2446. (c) Akita, M.; Yasuda, H.; Nagasuna, K.; Nakamura, A. *Bull. Chem. Soc. Jpn.* **1983**, *56*, 554−558. (d) Piers, W. E.; Shapiro, P. J.; Bunel, E. E.; Bercaw, J. E. *Synlett* **1990**, 74−84. (e) Bazan, G. C.; Rodriguez, G.; Ashe, A. J.; Al-Ahmad, S.; Kampf, J. W. *Organometallics* **1997**, *16*, 2492−2494. (f) Thiele, S.; Erker, G. *Chem. Ber.* **1997**, *130*, 201−207.
(12) (a) Piers, W. E.; Bercaw, J. E. *J. Am. Chem. Soc.* **1990**, *112*, 9406−9407. (b) Molander, G. A.; Hoberg, J. O. *J. Am. Chem. Soc.* **1992**, *114*, 3123−3125. (c) Negishi, E.; Jensen, M. D.; Kondakov, D. Y.; Wang, S. *J. Am. Chem. Soc.* **1994**, *116*, 8404−8405. (d) Shaughnessy, K. H.; Waymouth, R. M. *J. Am. Chem. Soc.* **1995**, *117*, 5873−5874.
(13) (a) Bogdanovic, B.; Henc, B.; Karmann, H.-G.; Nüssel, H.-G.; Walter, D.; Wilke, G. *Ind. Eng. Chem.* **1970**, *62*, 34−44. (b) Bogdanovic, B. *Adv. Organomet. Chem.* **1979**, *17*, 105−140.
(14) Behr, A.; Freudenberg, U.; Keim, W. *J. Mol. Catal.* **1986**, *35*, 9−17.
(15) Walther, D.; Döhler, T.; Heubach, K.; Klobes, O.; Schweder, B.; Görls, H. *Z. Anorg. Allg. Chem.* **1999**, *625*, 923−932.
(16) Kisanga, P.; Goj, L. A.; Widenhoefer, R. A. *J. Org. Chem.* **2001**, *66*, 635−637.
(17) Bray, K. L.; Lloyd-Jones, G. C.; Munoz, M. P.; Slatford, P. A.; Tan, E. H. P.; Tyler-Mahon, A. R.; Worthington, P. A. *Chem.—Eur. J.* **2006**, *12*, 8650−8663.
(18) Tan, E. H. P.; Lloyd-Jones, G. C.; Harvey, J. N.; Lennox, A. J. J.; Mills., B. M. *Angew. Chem., Int. Ed. Engl.* **2009**, *48*, 6262−6265.
(19) Tan, E. H. P.; Lloyd-Jones, G. C.; Harvey, J. N.; Lennox, A. J. J.; Mills, B. M. *Angew. Chem., Int. Ed. Engl.* **2011**, *50*, 9602−9606.
(20) Nelson, B.; Hiller, W.; Pollex, A.; Hiersemann, M. *Org. Lett.* **2011**, *13*, 4438−4441.
(21) Schramm, R. F.; Wayland, B. B. *Chem. Commun.* **1968**, 898−899.
(22) A possible explanation of this experimental observation is that the generation of the active catalyst, likely a "L_nPd−H"-species, from the precatalyst requires residual quantities of water.
(23) Using $[Pd(MeCN)_4](BF_4)_2$ at ambient temperature, screening of various solvents ($PhCH_3$, $PhCF_3$, C_6F_6, CH_3NO_2, MeCN, THF, Et_2O) and an additive (CF_3CH_2OH) did not improve the chemoselectivity. We observed limited catalyst solubility in hydrocarbon solvents and low conversion rates in Lewis basic solvents.
(24) Lloyd-Jones, G., C.; Stephen, S., C. *Chem. Commun.* **1998**, 2321−2322.
(25) Sen, A.; Lai, T. W. *Organometallics* **1983**, *2*, 1059−1060.
(26) Attempts to isolate (crystallization) or characterize (NMR) Pd species from the reaction mixture were unsuccessful.
(27) See Computational Chemistry.
(28) We are grateful to a reviewer for his insightful comments.
(29) The cycloisomerization of **1b** using our standard protocol ($[Pd(MeCN)_4](BF_4)_2$, CH_2Cl_2, ambient temperature) at different concentrations (c = 0.5 M, 0.1 M, 0.01 M) did not alter the monomer/dimer ratio.
(30) The *E*-configuration of the C1/C2 double bond of **6b** was assigned on the basis of the ^{1}H NMR coupling constant of the vinylic protons (^3J = 15.3 Hz). The cycloisomerization/dimerization of (±)-*syn*-**1b** could generate up to four racemic diastereomers. Notably, only two major diastereomers were detected by ^{1}H NMR spectroscopy. In those cases, where the assignment of the relative configuration of the dimers was successful, we observed a 2′,3′-*cis*-relationship.

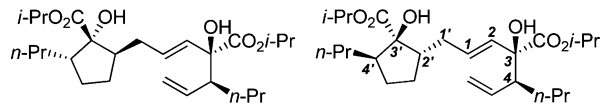

(±)-2′,3′-*trans*-**6b**

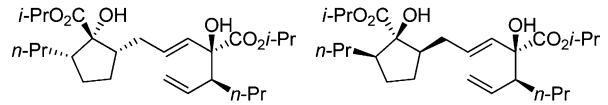

(±)-2′,3′-*cis*-**6b**

(31) The cycloisomerization/dimerization/cycloisomerization of (±)-*syn*-**1b** could generate up to eight racemic diastereomers. Notably, only two diastereomers of (±)-**7b** were detected. The major diastereomer could be isolated and fully characterized, and its all-*cis* configuration was verified by 2D NOESY experiments; in accordance with the assumed S_2 (enantiotopic atoms or groups of atoms) *or* C_2 symmetry (homotopic atoms or groups of atoms) of this diastereomer of (±)-**7b**, the corresponding NMR spectra display a half set of resonances.

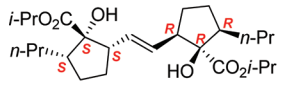

7b (S_2)

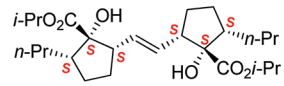

(±)-**7b** (C_2)

(32) See the Supporting Information for Ortep presentation; CCDC 868298 contains the supplementary crystallographic data for this contribution. These data can be obtained free of charge from The Cambridge Crystallographic Data Centre via www.ccdc.cam.ac.uk/data_request/cif.
(33) (a) Beesley, R. M.; Ingold, C. K.; Thorpe, J. F. *J. Chem. Soc., Trans.* **1915**, *107*, 1080−1106. (b) Sammes, P. G.; Weller, D. J. *Synthesis* **1995**, 1205−1222. (c) Jung, M. E.; Piizzi, G. *Chem. Rev.* **2005**, *105*, 1735−1766.
(34) See the Supporting Information for Ortep presentation; CCDC 868297 contains the supplementary crystallographic data for this contribution. These data can be obtained free of charge from The Cambridge Crystallographic Data Centre via www.ccdc.cam.ac.uk/data_request/cif.
(35) Frisch, M. J.; et al. *Gaussian 03*, Revision E.01; Gaussian, Inc.: Wallingford CT, 2004. Full reference given in the Supporting Information.
(36) (a) Becke, A. D. *J. Chem. Phys.* **1993**, *98*, 5648−5652. (b) Lee, C. T.; Yang, W.; Parr, R. G. *Phys. Rev. B* **1988**, *37*, 785−789.

(c) Miehlich, B.; Savin, A.; Stoll, H.; Preuss, H. *Chem. Phys. Lett.* **1989**, *157*, 200−206.
(37) Friesner, R. A.; Murphy, R. B.; Beachy, M. D.; Ringnalda, M. N.; Pollard, W. T.; Dunietz, B. D.; Cao, Y. *J. Phys. Chem. A* **1999**, *103*, 1913−1928.
(38) (a) Weigend, F.; Ahlrichs, R. *Phys. Chem.* **2005**, *7*, 3297−3305. (b) Andrae, D.; Häußermann, U.; Dolg, M.; Stoll, H.; Preuß, H. *Theor. Chim. Acta* **1990**, *77*, 123−141.
(39) Peterson, K. A.; Figgen, D.; Goll, E.; Stoll, H.; Dolg, M. *J. Chem. Phys.* **2003**, *119*, 11113−11123.
(40) In context of diene-cycloisomerization/polymerization, a number of similar Pd^{II}-O-donor-chelate complexes, acting as resting states for these transformations, have been described in the literature: (a) Goj, L. A.; Widenhoefer, R. A. *J. Am. Chem. Soc.* **2001**, *123*, 11133−11147. (b) Goj, L. A.; Cisneros, G. A.; Yang, W.; Widenhoefer, R. A. *J. Organomet. Chem.* **2003**, *687*, 498−507. (c) DiRenzo, G. M.; White, P. S.; Brookhart, M. *J. Am. Chem. Soc.* **1996**, *118*, 6225−6234. (d) Margl, P.; Ziegler, T. *J. Am. Chem. Soc.* **1996**, *118*, 7337−7344. (e) Mecking, S.; Johnson, L. K.; Wang, L.; Brookhart, M. *J. Am. Chem. Soc.* **1998**, *120*, 888−899. (f) Perch, N. S.; Widenhoefer, R. A. *Organometallics* **2001**, *20*, 5251−5253. (g) Nakamura, A.; Munakata, K.; Ito, S.; Kochi, T.; Chung, L. W.; Morokuma, K.; Nozaki, K. *J. Am. Chem. Soc.* **2011**, *133*, 6761−6779. (h) Perch, N. S.; Widenhoefer, R. A. *J. Am. Chem. Soc.* **2004**, *126*, 6332−6346.
(41) We were unable to locate a static stationary point between **TS(M11−M13)** and **M13**.
(42) (a) Hiersemann, M. *Tetrahedron* **1999**, *55*, 2625−2638. (b) Hiersemann, M.; Lauterbach, C.; Pollex, A. *Eur. J. Org. Chem.* **1999**, 2713−2724. (c) Hiersemann, M. *Synlett* **2000**, 415−417. (d) Hiersemann, M. *Eur. J. Org. Chem.* **2001**, 483−491. (e) Hiersemann, M.; Abraham, L.; Pollex, A. *Synlett* **2003**, 1088−1095.
(43) Juaristi, E.; Martinez-Richa, A.; Garcia-Rivera, A.; Cruz-Sanchez, J. S. *J. Org. Chem.* **1983**, *48*, 2603−2606.
(44) Kirsten, M.; Rehbein, J.; Hiersemann, M.; Strassner, T. *J. Org. Chem.* **2007**, *72*, 4001−4011.
(45) Rehbein, J.; Leick, S.; Hiersemann, M. *J. Org. Chem.* **2009**, *74*, 1531−1540.
(46) Hiersemann, M. *Synthesis* **2000**, 1279−1290.
(47) Sen, A.; Lai, T. W. *Organometallics* **1983**, *2*, 1059−1060.
(48) (a) Schramm, R. F.; Wayland, B. B. *Chem. Commun.* **1968**, 898−899. (b) Lai, T. W.; Sen, A. *Organometallics* **1984**, *3*, 866−870.

dx.doi.org/10.1021/jo3004088 | *J. Org. Chem.* XXXX, XXX, XXX−XXX